

Unbiased placental secretome characterization identifies candidates for pregnancy complications

Tina Napso

Centre for Trophoblast Research

Xiaohui Zhao

Centre for Trophoblast Research <https://orcid.org/0000-0001-9922-2815>

Marta Ibanez Lligona

Centre for Trophoblast Research

Ionel Sandovici

University of Cambridge <https://orcid.org/0000-0001-5674-4269>

Richard Kay

Institute of Metabolic Science

Fiona Gribble

Institute of Metabolic Science <https://orcid.org/0000-0002-4232-2898>

Frank Reimann

University of Cambridge <https://orcid.org/0000-0001-9399-6377>

Claire Meek

Institute of Metabolic Science

Russell Hamilton

University of Cambridge <https://orcid.org/0000-0002-0598-3793>

Amanda Sferruzzi-Perri (✉ ans48@cam.ac.uk)

Centre for Trophoblast Research <https://orcid.org/0000-0002-4931-4233>

Article

Keywords:

Posted Date: September 2nd, 2020

DOI: <https://doi.org/10.21203/rs.3.rs-60422/v1>

License: © ⓘ This work is licensed under a Creative Commons Attribution 4.0 International License.

[Read Full License](#)

Version of Record: A version of this preprint was published at Communications Biology on June 8th, 2021. See the published version at <https://doi.org/10.1038/s42003-021-02214-x>.

1 **Unbiased placental secretome characterization identifies candidates for pregnancy complications**

2 Napso T¹, Zhao X¹, Ibañez Lligoña M¹, Sandovici I^{1,2}, Kay RG³, Gribble FM³, Reimann F³, Meek CL³,
3 Hamilton RS^{1,4}, Sferruzzi-Perri AN^{1*}.

4
5 Running title: Placenta secretome identifies pregnancy biomarkers

6
7 ¹Centre for Trophoblast Research, Department of Physiology, Development and Neuroscience,
8 University of Cambridge, Cambridge, UK.

9 ²Metabolic Research Laboratories, MRC Metabolic Diseases Unit, Department of Obstetrics and
10 Gynaecology, The Rosie Hospital, Cambridge, UK.

11 ³Wellcome-MRC Institute of Metabolic Science, Addenbrooke's Hospital, Cambridge, UK.

12 ⁴Department of Genetics, University of Cambridge, Cambridge, UK.

13
14 *Author for correspondence:

15 Amanda N. Sferruzzi-Perri

16 Centre for Trophoblast Research,

17 Department of Physiology, Development and Neuroscience,

18 University of Cambridge,

19 Cambridge, UK CB2 3EG

20 ans48@cam.ac.uk

21
22
23 **Abstract**

24 Alterations in maternal physiological adaptation during pregnancy lead to complications, including
25 abnormal birthweight and gestational diabetes. Maternal adaptations are driven by placental
26 hormones, although the full identity of these is lacking. This study unbiasedly characterised the
27 secretory output of mouse placental endocrine cells and examined whether these data could identify
28 placental hormones important for determining pregnancy outcome in humans. Secretome and cell
29 peptidome analyses were performed on cultured primary trophoblast and fluorescence-activated
30 sorted endocrine trophoblasts from mice and a placental secretome map was generated.
31 Bioinformatic analyses showed that placental secretome proteins are involved in metabolic, immune
32 and growth modulation, are largely expressed by human placenta and several are dysregulated in

33 pregnancy complications. Moreover, proof-of-concept studies found that secreted placental proteins
34 (sFLT1/MIF and ANGPT2/MIF ratios) were increased in women prior to diagnosis of gestational
35 diabetes. Thus, placental secretome analysis could lead to the identification of new placental
36 biomarkers of pregnancy complications.

37

38 **Introduction**

39 The placenta forms the functional interface between the mother and fetus that is essential for fetal
40 development and growth during pregnancy. It is responsible for secreting a plethora of endocrine
41 mediators that induce local and systemic changes in the mother to enable fetal nutrient and oxygen
42 transfer and prevent immunological rejection of the fetus¹. Aberrant placental function can lead to
43 insufficient or inappropriate adaptations in maternal physiology, with consequences for pregnancy
44 outcome and with immediate and lifelong impacts on the health of both the mother and child. Indeed,
45 placental malfunction is a leading cause for the development of pregnancy complications, such as
46 preeclampsia (PE), gestational diabetes mellitus (GDM) and intrauterine growth restriction (IUGR).
47 Combined, these complications affect up to 6-8% of pregnancies in the UK
48 (<https://www.gov.uk/government/statistics/birth-characteristics-england-and-wales-2014>).

49 Typically, these complications are diagnosed in the second or even the third trimester of gestation,
50 after the complication has already manifested. Moreover, current diagnosis methods, namely blood
51 pressure and proteinuria evaluation for PE, oral glucose tolerance test for GDM and uterine fundal
52 height and ultrasound measures for IUGR are performed at a specific time/s in gestation and the
53 development of the complication may not be detected in some cases. Therefore, the identification of
54 novel placental biomarkers for earlier detection and improved diagnosis of pregnancy complications
55 is highly desirable. Moreover, the illumination of placental biomarkers may aid in the design of novel
56 therapeutic targets for pregnancy complications.

57

58 The notion that placental biomarkers may provide diagnostic or prognostic value for pregnancy
59 complications is a long-standing and supported concept. For instance, detection of the placental
60 hormone, chorionic gonadotropin is used to confirm pregnancy, reduced levels of pregnancy-
61 associated plasma protein-A (PAPP-A) in the maternal circulation are predictive of IUGR and PE² and
62 an imbalance in placental derived angiogenic regulators, like soluble fms-like tyrosine kinase 1 (sFLT1)
63 and placental growth factor (PlGF) can be predictive of PE³. However, studies in experimental animals
64 have demonstrated that the production of many other protein hormones by the placenta could also

65 be important in determining pregnancy outcome^{1,4}. In rodents, placental lactogens/prolactins
66 (PL/PRL), growth hormone (GH) and insulin-like growth factor 2 (IGF2) modulate maternal insulin and
67 glucose levels during pregnancy and perturbed expression of these proteins by the placenta have been
68 associated with GDM and abnormal fetal growth in humans. The placenta also produces a wide variety
69 of cytokines throughout pregnancy, which contribute to the low grade systemic inflammation and
70 induction of maternal insulin resistance that normally occurs in the second half of pregnancy and some
71 data suggest that placental cytokine production is aberrant in women with poor pregnancy outcomes
72 like PE, GDM and IUGR⁵. Additionally, the placenta secretes inhibins, activins and relaxins, which aid
73 in the adaptation of the endocrine, renal, circulatory and immune systems of the mother during
74 gestation¹. Finally, the placenta secretes proteases, inhibitors of peptidases, binding proteins and
75 soluble forms of receptors for steroids, growth factors, cytokines and circulating factors, like
76 lipoproteins, which contribute to the pleiotropic endocrine regulation of maternal physiology during
77 gestation and show some predictive value for conditions like IUGR⁶⁻⁸. Thus, there is likely a
78 constellation of protein mediators secreted by the placenta that facilitate maternal adaptations and
79 ensure adequate fetal growth, required for a healthy pregnancy outcome.

80

81 Transcriptomic analyses has informed on the repertoire of hormones expressed by the human
82 placenta in healthy and complicated pregnancies⁹⁻¹². However, these studies are conducted mainly on
83 samples obtained at delivery and involve analysis of pieces of placenta tissue, which is heterogeneous
84 in nature and includes trophoblast, vascular, stromal and specialised immune cell types. Moreover, as
85 powerful a tool it may be, transcriptomic analyses on their own may not be sufficient to identify the
86 protein hormones secreted by the placenta. This is because genes can be subjected to post-
87 transcriptional and post-translational regulatory mechanisms, such as alternative splicing, folding,
88 transport, localization, degradation and secretion. Thus, analysis of the secretome, the complete list
89 of proteins secreted by the placenta, would be invaluable for identifying placental biomarkers of
90 maternal and fetal wellbeing that could be altered prior to the manifestation of a pregnancy
91 complication.

92

93 The mouse is a valuable species for defining the placental secretome. This is because hormone
94 secretion by the placenta is principally performed by trophoblast endocrine cells that are conveniently
95 arranged into a structure, termed the junctional zone. The junctional zone is also discrete from, and
96 forms under distinct genetic instruction to, the labyrinthine zone, which performs substrate transport
97 function in the mouse placenta. This is in contrast to humans, where the endocrine and transport

98 functions of the placenta are carried out by the same region/cell type, the syncytiotrophoblast (STB),
99 preventing the specific, sole examination of placental hormone production. The mouse also offers the
100 key advantage that tools to selectively modify and isolate endocrine cells in the placenta are now
101 available¹³. Moreover, despite some variations between mice and humans, many mouse-specific
102 hormone genes are structurally similar to those in the human and perform similar functions (e.g.
103 PRL/PL and GH genes)¹. Furthermore, many gene and protein networks regulating placental
104 development and function overlap in the two species^{14,15}.

105

106 Herein, we first established a method for obtaining primary cultures of mouse placental endocrine
107 cells from which the cells and secretory output could be collected. As a complementary approach, we
108 also employed fluorescence-activated cell sorting (FACS) to isolate endocrine cells from the placenta
109 of mice. We used mass spectrometry to unbiasedly identify the proteins in our different mouse
110 placental endocrine cell preparations and applied a bioinformatic pipeline to refine a placental
111 secretome map. We then overlaid our placental secretome map to a compilation of RNA/protein
112 expression databases publicly available for the human placenta in women with pregnancy
113 complications, including PE, GDM and IUGR to identify secreted placental proteins that could be
114 clinically important. As a proof of concept, we quantified the abundance of four secreted placental
115 protein candidates (sFLT1, MIF, ANGPT2 and IGF2) and their ratios to one another in blood samples
116 taken from women who had uneventful/healthy pregnancy outcomes and those who developed GDM
117 (both populations were normotensive). We found that sFLT1 was altered in abundance in women with
118 GDM and moreover, the ratios of sFLT1 or ANGPT2 to MIF were altered in the first trimester of
119 pregnancy in women who went on to develop and be diagnosed with GDM in the second trimester of
120 pregnancy. Finally, we identified several transcription factors that are predicted to be important for
121 controlling endocrine function of the placenta and determining pregnancy outcome. Our methodology
122 and novel placental secretome map may be useful in identifying additional placental biomarkers for
123 pregnancy complications.

124

125 **Results:**

126 We first wanted to establish a method for obtaining primary cultures of mouse placental endocrine
127 cells from which secretory output could be collected and unbiasedly characterised. We harvested
128 placentas at day 16 of gestation from wild-type females mated with males expressing Cre-EGFP under
129 the *Tpbpa* promoter, which is specifically active in the trophoblast endocrine cells of the junctional

130 zone¹³ (Figure 1A). Day 16 of gestation was chosen as this corresponds to when all the endocrine cells
131 in the mouse placenta have differentiated and are non-proliferating. Moreover, this is when the
132 junctional zone is largest in absolute terms. The *Tpbpa*-Cre-EGFP reporter was used to visualise the
133 trophoblast endocrine cells, which were found to be enriched in the second layer of our Percoll
134 gradient (between 1.028 and 1.050 g/ml; Figure 1A&B). Trophoblast cells from this layer were then
135 cultured for up to 120h and the optimal time point for secretome analysis was identified to be 48h
136 based on dynamics of trophoblast density (*Krt18* expression) and the levels of viability (XTT levels),
137 necrosis (LDH levels) and apoptosis markers (*p53* and *Bax* expression) throughout the culturing (Figure
138 1C). As expected, the 48h primary cultures contained a high density of endocrine trophoblasts, as
139 indicated by the high expression of *Tpbpa* and comparatively very low expression of the transport
140 labyrinth zone marker, *Mct4* (Figure 1D). These cultures contained all three types of junctional zone
141 cells, *i.e.* the endocrine spongiotrophoblasts, glycogen cells and giant cells, as evidenced by the
142 expression of their unique gene markers *Prl8a8*, *Gjb3* and *Hand1*, respectively (Figure 1E&F).

143

144 **Peptidome and secretome analysis of primary cultured trophoblast cells from mouse placenta**

145 We then determined the secretome of our primary mouse trophoblast endocrine cell cultures. This
146 involved performing LC-MS/MS on both the cells and conditioned medium from the cultures at 48h
147 and then applying a bioinformatics pipeline (Figure 1G). We identified a total of 1,534 and 1,445
148 proteins in the cells and conditioned medium of the cultures, respectively. After considering only
149 proteins that were detected in 4 out of 5 samples, protein lists were then converted to their
150 corresponding gene ID and expression by the mouse placenta verified using publicly available RNA
151 datasets (Supplementary Table 1). As we wanted to ultimately translate our findings from the mouse
152 to humans, we additionally overlaid our converted mouse gene lists with publicly available RNA
153 datasets for the human placenta (Supplementary Table 1) and performed systematic orthologue
154 searches. To further refine our lists to secreted proteins, we applied SignalP and gene ontology
155 analysis to capture proteins that employ both the "conventional", as well as "unconventional"
156 secretion pathways (see methods for details). This resulted in a refined list of 158 and 257 secreted
157 proteins detected in the cultured cells and conditioned medium (110 were common between the
158 sample types), respectively that are expressed by both the mouse and human placenta. Reactome
159 pathway analysis revealed that the proposed functions of secreted proteins in the cultured cells and
160 conditioned medium were largely similar, with the highest scoring pathways including those involved
161 in the immune system, neutrophil degranulation, homeostasis and insulin-like growth factor (IGF)
162 regulation (Fig. 1H and G). All data outputs at each step of the pipeline, including the proteins/genes

163 expressed in the mouse but not the human placenta can be found in GitHub (<https://github.com/CTR->
164 [BFX/2020-Napso_Sferruzi-Perri](https://github.com/CTR-BFX/2020-Napso_Sferruzi-Perri)).

165

166 **Peptidome and secretome analysis of sorted endocrine cells from the mouse placenta**

167 As a complementary approach to the primary trophoblast cultures, endocrine cells from the mouse
168 placenta on day 16 of pregnancy were isolated using FACS. This was performed by mating the *Tpbpa*-
169 Cre-EGFP mouse line to the double-fluorescent Cre reporter line, mTmG¹⁶ (Figure 2A). As expected,
170 placentas obtained from these matings showed EGFP in the junctional zone of the placenta, whereas
171 the labyrinth, decidua and fetus were positive for tdTom (Figure 2B,C). Moreover, sorting the EGFP-
172 positive cells provided us with highly enriched isolates of junctional zone cells (as indicated by the high
173 expression of *Tpbpa*, with little to low detection of the *Mct4* gene; Figure 2D) containing the three
174 major endocrine cell types of the mouse placenta (Figure 2E). Using LC-MS/MS we identified a total of
175 1,142 proteins in the sorted placental endocrine cells (Figure 2F). Applying a similar pipeline to the
176 analysis of cultured placental endocrine cells, we narrowed down our list of proteins obtained in the
177 sorted placental endocrine cells to 105 secreted proteins that are shared between the mouse and
178 human placenta (Figure 2F). Gene ontology analysis indicated that these secreted placental proteins
179 function in pathways related to the immune system, neutrophil degranulation and metabolism of
180 proteins, among others (Figure 2G). All data outputs at each step of the pipeline, including the
181 proteins/genes expressed in the mouse but not the human placenta can be found in GitHub
182 (https://github.com/CTR-BFX/2020-Napso_Sferruzi-Perri). Proteins detected in the sorted placental
183 endocrine cells that were not predicted to be secreted were analysed by gene ontology analysis. This
184 revealed that many proteins detected are proposed to play roles in protein synthesis, translation and
185 metabolism, amongst others and are in line with their possible regulatory role in modulating the
186 function of placental endocrine cells (Supplementary Figure 1 and Supplementary Table 3).

187

188 **Creating a placental secretome map**

189 Given that the LC-MS/MS method is unbiased, but cannot exhaustively characterize the entire
190 proteome of a given set of samples, we then combined the lists of secreted placental proteins
191 expressed by mouse and human placenta obtained using the two methods presented above, to
192 generate a more comprehensive placental secretome map (Figure 3A). This approach resulted in a
193 total of 319 secreted proteins that are expressed by both mouse and human placenta (Figure 3A) and
194 another 31 that are specific to the mouse (Supplementary Figure 2). We aligned our list of 319 secreted

195 placental proteins with data from single-cell RNA-Seq analysis of the human placenta at 8 and 24
196 weeks of gestation¹⁷ and found that 94% of our proteins (299 out of 319) were expressed in the STB
197 (Figure 3B and F). We also aligned our list of 319 secreted placental proteins with data on the
198 conditioned media from trophoblast organoids prepared from first trimester human placenta¹⁸ and
199 identified 56 secreted placental proteins in common (Figure 3B). Gene ontology analysis of the
200 complete list of 319 proteins/genes demonstrated that they play roles in the response to stimuli and
201 stress and regulation of organismal process (Figure 3C). Moreover, many placental proteins identified
202 are implicated in protein and signalling receptor binding and contain protein-interacting domains,
203 such as serpin, conserved sites and the EGF-like domains, observations which are overall consistent
204 with the notion that they are secreted (Figure 3C). Using gene expression enrichment analysis for
205 mouse and human tissues, we found that 20 of the proteins were highly expressed (>10 fold) in the
206 mouse placenta compared to other tissues (Figure 3D) and 4 secreted placental proteins, TFPI2,
207 SERPINE2, IGF2 and FLT1 were enriched in the human placenta compared to other tissues (Figure 3E).
208 Further alignment of our complete list of secreted placental proteins with single-cell RNA-Seq analysis
209 of the human placenta revealed that several proteins were enriched predominantly in the STB,
210 including FLT1, TFPI2 and ANGPT2 (Figure 3F). Moreover, all the proteins that we identified are
211 reported to be expressed by the syncytiotrophoblast (STB), extravillous cytotrophoblast (EVT) or
212 cytotrophoblast (CTB) of the human placenta.

213

214 **Placental secretome map is enriched in proteins that are differentially expressed in human** 215 **pregnancy complications**

216 We wanted to know whether our novel placental secretome map could help us to identify placental
217 proteins that may serve as circulating biomarkers/diagnostic indicators of maternal and fetal
218 wellbeing in human pregnancy. We collated publicly available RNA and protein expression datasets
219 for the human placenta from pregnancies complicated by PE, GDM, IUGR, small for gestational age
220 (SGA) and large of gestational age (LGA) (Supplementary Table 2). We then overlaid our placental
221 secretome map to our collated database of placental RNA/protein expression for these pregnancy
222 complications (Supplementary Table 2). This identified 119 secreted proteins that were dysregulated
223 in the human placenta in the pregnancy complications studies (Figure 4A). There was some overlap in
224 the expression of secreted placental proteins between pregnancy complications and, aside from LGA,
225 all complications showed an altered expression of ANGPT2, FLT1, IGF2 and TIMP2 (Figure 4A). Of note,
226 FLT1 and IGF2 are particularly enriched in the human placenta compared to other tissues (see also
227 Figure 3F). Furthermore, we found several secreted placental proteins that were uniquely altered in

228 specific pregnancy complications. For instance, we found 18 secreted placental proteins that were
229 only altered in the placenta of women with GDM, 47 specifically altered in PE and 5 uniquely altered
230 in IUGR pregnancies (Figure 4A). Of those uniquely altered in PE and IUGR, secreted placental proteins
231 TFPI2 and SERPINE2, respectively, are reported to be highly enriched in the human placenta compared
232 to other tissues. GO analysis revealed that secreted placental proteins uniquely altered in GDM are
233 involved in the metabolism of proteins and extracellular matrix organisation (Supplementary Table 4-
234 A), those altered in PE largely function in the immune system and platelets (Supplementary Table 4-
235 B) and those changed in IUGR are implicated in fibril, collagen and laminin formation (Supplementary
236 Table 4-C).

237

238 **MIF/sFLT1 and ANGPT2/MIF ratios are altered in human GDM blood samples**

239 We wanted to know whether our secretome map may be useful in identifying placental biomarkers
240 that could be measured in the circulation of women and aid in the detection of a pregnancy
241 complication. To test this possibility, we analysed the abundance of secreted placental proteins in
242 blood taken from women at booking (12 weeks of gestation) and after glucose tolerance testing (28
243 weeks of gestation) who were subsequently classified as normoglycemic or diagnosed with GDM.
244 Maternal clinical characteristics and pregnancy outcomes for the women with normal glucose
245 tolerance or GDM are shown in Table 1. We quantified the abundance of the following secreted
246 placental proteins, sFLT1, ANGPT2, MIF and IGF2 as they were highly enriched in human placenta
247 and/or differentially altered in several pregnancy complications (Figure 4A). We first visualised the cell
248 specific expression of these proteins at the maternal–fetal interface in early human pregnancy using
249 the CellxGene tool (<https://maternal-fetal-interface.cellgeni.sanger.ac.uk/>)¹⁹. FLT1 was shown to be
250 highly and mainly expressed in syncytiotrophoblast and extravillous trophoblasts (Figure 4B), whilst
251 ANGPT2, MIF and IGF2 were more broadly expressed by trophoblast cell populations (Supplementary
252 Figure 3). All four secreted placental proteins were detectable in the maternal circulation as early as
253 12 weeks of gestation (Figure 4C and Supplementary Figure 4). Furthermore, several showed changes
254 in abundance with gestational age and in those women who developed GDM. ANGPT2 and MIF
255 declined in the maternal circulation between 12 and 28 weeks of gestation, in line with the reduction
256 in placental expression indicating that the placenta is the main source (Fig 3F). However the decline
257 in MIF with gestational age was not observed in women who developed GDM (due, in part to non-
258 significantly lower values in GDM versus healthy women at 12 weeks). Moreover, sFLT1 circulating
259 levels were overall, significantly elevated in the circulation of women with GDM diagnosis ($p=0.05$). In
260 contrast, IGF2 levels in the maternal circulation were not significantly different between 12 and 28

261 weeks of gestation or in women who developed GDM (Figure 4C and Supplementary Figure 4). As
262 pregnancy complications can be caused by an alteration of several pathways and biological systems,
263 it is common to evaluate the relationship between the abundance of different biomarkers. We found
264 that the ratio of sFLT1 to MIF concentration was increased by 210% ($p=0.0003$) and ANGPT2 to MIF
265 was increased by 97% ($p=0.02$) in women at 12 weeks of gestation who went on to develop GDM
266 compared to the healthy pregnancies (Figure 4D).

267

268 **A transcriptional network controlling placental proteome highlights links with pregnancy** 269 **complications**

270 We wanted to gain further information on the regulation of placental endocrine function and its
271 significance for determining pregnancy outcome. To this aim, we searched for transcription factors
272 (TFs) that had significant enrichment of binding sites at the promoters of genes encoding the 319
273 proteins in our placental secretome map (Figure 3A). We used two computational tools, Analysis of
274 Motif Enrichment and Ingenuity Pathway Analysis and identified 33 common TFs expressed by
275 trophoblast cells in human placenta and controlling the expression of a total of 96 proteins from our
276 placental secretome map (Supplementary Table 5). All of these TFs were expressed by the STB at 8
277 weeks of gestation, when their placental secreted targets were too. Furthermore, the expression of
278 10 of these TFs has been reported to be perturbed in human pregnancy complications (Figure 5A).
279 These 10 TFs control the expression of 36 members of the placental proteome map, 20 of which are
280 reported to be differentially expressed in human pregnancy complications (Figure 5B). Of note was
281 ARNT2, which is reported to be dysregulated in PE and IUGR and implicated in the control of 10 genes
282 encoding proteins in the placental secretome, of which 5 were further reported to be altered in
283 pregnancy complications (Supplementary Table 5). PLAG1 and CREB1 were specifically altered in the
284 placenta from women with GDM and proposed to be key in regulating of placental secreted proteins
285 like IGF2 and FLT1, which were also identified as altered in expression in such pregnancies. FOS, MYCN
286 and NFYC were found to be altered in PE pregnancies and are predicted to modulate the gene
287 expression of up to 11 proteins in our secretome list that are also reported to be differentially
288 expressed in PE (Figure 5A and Supplementary Table 5).

289

290 **Discussion**

291 Our study has established a comprehensive secretome map of the placenta. By utilising transgenic
292 mouse lines for tracking placental endocrine cells, together with advanced molecular techniques and

293 bioinformatics analysis, we have characterized a placental secretome map relevant for both mouse
294 and human pregnancy. To achieve this, we performed mass spectrometry on three types of samples,
295 i) primary cultures containing mouse placental endocrine cells, ii) conditioned media from primary
296 cultures of mouse placental endocrine cells and iii) endocrine cells isolated from the mouse placenta
297 by fluorescence-activated cell sorting. A robust bioinformatics pipeline was then used to integrate our
298 proteins lists and to include in our analysis only proteins expressed by both the mouse and human
299 placenta, as well as those destined to be secreted. By overlaying our secretome map to publicly
300 available datasets for the human placenta, we were able to identify that several secreted placental
301 proteins were altered in pregnancy complications including GDM, PE and IUGR. Moreover, in proof of
302 concept experiments using blood samples from women who were healthy or developed GDM, our
303 findings suggest that the relative abundance of secreted placental candidates identified using our
304 secretome map, may be altered as early as week 12 of gestation, which predates traditional clinical
305 diagnosis at 24 weeks. Lastly, we identified transcription factors that are likely to govern the
306 expression of placental hormones with important implications for pregnancy outcome. Taken
307 together, our data demonstrate that our methodology and placental secretome map may illuminate
308 promising biomarker candidates as early diagnostic indicators and therapeutic targets for pregnancy
309 complications linked to placental malfunction. Moreover, our methodology and findings may have
310 relevance for understanding the significance of placental endocrine function in mammalian
311 development and pregnancy physiology, more broadly.

312

313 Three parallel approaches were used to obtain lists of secreted placental proteins that could be
314 integrated as a secretome map. This was fundamentally important, as we wanted to maximise our
315 ability to detect secreted placental proteins without being limited by sample preparation, method
316 sensitivity and specificity. We adapted published methods²⁰ and used the *Tpbpa*-Cre-EGFP mouse
317 line¹³ to obtain primary cell cultures containing a high density of mouse placental endocrine cells. By
318 monitoring the behaviour of our cultured cells, we were able to show that at 48h of culture, cell
319 viability was stable, with no increase in cell necrosis or cell death. Furthermore, at 48h, our primary
320 cell cultures contained the three main endocrine cell types of the mature mouse placenta. We
321 analysed the cultured cells and conditioned media separately, as proteins can be secreted at low
322 concentrations into the culture media, resulting in recovery difficulties. Moreover, salts and other
323 compounds in the media may interfere with protein detection. Furthermore, highly abundant proteins
324 can mask the detection of lowly expressed proteins, resulting in selective detection or a mis-
325 representation of the proteome when analysing cultured cells. To further increase the sensitivity of
326 detecting secreted placental proteins, we concentrated the conditioned media of our primary cell

327 cultures prior to mass spectrometry and likely due to this, we obtained a larger list of secreted
328 placental proteins from the conditioned media (26 proteins in the mouse and 257 in mouse and
329 human) compared to the cultured cells (5 proteins in mouse and 158 in mouse and human). However,
330 our primary placental endocrine cell cultures were not pure, and cells may alter their protein
331 expression when cultured. As a complementary approach, we also identified the proteins in freshly
332 isolated mouse placental endocrine cells using the *Tpbpa*-Cre-EGFP and mTmG murine lines and
333 fluorescence-activated cell sorting. This approach delivered highly pure samples containing all three
334 placental endocrine lineages. However, some trophoblast giant cells in the mouse placenta may have
335 been lost due to size limitation of the nozzle for the fluorescence-activated cell sorting (100µm).
336 Moreover, both the preparation of primary cultures and fluorescence-activated sorting of mouse
337 placental endocrine cells resulted in a relatively lower abundance of glycogen cells than expected for
338 the mouse placenta at day 16 (normally the relative proportion of endocrine cell types is
339 spongiotrophoblast > glycogen cells > trophoblast giant cells). This is somewhat expected, as glycogen
340 cells are sensitive to lysis and may thus be particularly sensitive to the sample preparation technique.
341 Nevertheless, 112 secreted placental proteins (7 proteins in mouse and 105 in mouse and human)
342 were detected in the pure placental endocrine cell isolates, of which 82% were also found in cultured
343 cells. Reactome pathway analysis of individual protein lists revealed that the proposed functions of
344 secreted proteins in the cultured cells, conditioned culture media and placental endocrine cell isolates
345 were overall similar, with the highest scoring pathways including those related to the immune system,
346 homeostasis and insulin-like growth factor (IGF) regulation. However, several of the proteins detected
347 were specific to one approach/sample type, which reinforces our approach of combining different
348 sample types/methodologies to optimise and broaden the detection of proteins secreted by the
349 placenta. Indeed, the combination of the three methodologies enabled the creation of map of 319
350 secreted proteins expressed by both mouse and human placenta and another 31 specific to the
351 mouse.

352

353 Of the 319 secreted placental proteins in mouse and human, 56 were previously reported to be
354 secreted from first trimester human trophoblast organoids¹⁸, including progranulin (GRN), insulin-like
355 growth factor II (IGF2), insulin-like growth factor-binding protein 2 (IBP2) and macrophage migration
356 inhibitory factor (MIF). Moreover, the majority of the proteins (300 out of 319) were localised to the
357 syncytiotrophoblast of the human placenta¹⁷, which is in direct contact with maternal blood and the
358 primary site for hormone production in the human placenta. The predominate localisation of proteins
359 in our secretome map to the syncytiotrophoblast in humans validates our method and highlights how
360 data generated may improve our understanding of the role and regulation of human placental

361 endocrine function. More than 60% of the proteins in our placental secretome map were predicted to
362 function in “response to stimulus”. This GO term includes secondary biological groups such as
363 regulation of signal transduction downstream of the interleukin-1 receptor type 2 (IL1R2),
364 macrophage metalloelastase (MMP12) and apolipoprotein A-I (APOA1) that participate in the
365 response to cytokines. It also included insulin-like growth factor-binding proteins (IGFBP2, IGFBP4 and
366 IGFBP6), which modulate the mitogenic and metabolic actions of insulin-like growth factors that play
367 important roles in pregnancy physiology²¹. Indeed, several of these proteins have been previously
368 shown to be secreted from the human placenta, such as the IL1R2²², IGF2 and IGFBPs²³, MMP12²⁴ and
369 APOA1²⁵ and are consistent with our findings. Many of the proteins in our secretome map were also
370 identified to be hormone binding proteins, or proteins that regulate signalling downstream of
371 receptors. These included annexin A5 (ANXA5) an anticoagulant protein, inhibin beta A chain (INHBA),
372 which is a subunit of both inhibin and activin, transthyretin (TTHY) a thyroid hormone-binding protein,
373 insulin-degrading enzyme (IDE), which binds to insulin and leukaemia inhibitory factor receptor (LIFR).
374 Whilst proteins like ANXA5, inhibins/activins, TTHY and LIFR have been previously reported to be
375 secreted from the placenta^{1,26-28}, we are not aware of any studies describing the secretion of other
376 proteins, like IDE from the human placenta. Furthermore, other secreted proteins such as adipocyte
377 enhancer-binding protein 1 (AEBP1) and Y-box-binding protein 1 (YBOX1), which can regulate
378 transcription were also detected in the placental secretome. Again however, to date, there are no
379 studies related to the secretion of AEBP1 and YBOX1 from the human placenta. Collectively our
380 findings may suggest that the secretome map comprises known and novel secreted placental proteins.

381

382 Two main protein domains featured in our placental secretome map were the “Serpin conserved site”
383 and the “EGF-like domain” which are important in regulating inflammatory processes, growth factor
384 signalling and extracellular matrix and cytoskeletal remodelling. Thus, in addition to identifying
385 proteins secreted by the placenta with systemic actions, proteins in our secretome map may also play
386 local autocrine and paracrine roles in modulating processes at the fetal-maternal interface, including
387 decidual remodelling/function, immune tolerance and placentation. Using tissue gene expression
388 enrichment analysis, we found that of the proteins in our placental secretome map, 20 were most
389 abundantly expressed by the placenta in mouse and 4 were enriched in the placenta in human. Of
390 note, TFPI2 a plasmin-mediated matrix remodelling, FLT1 a receptor for vascular endothelial growth
391 factor and proteins from the SERPIN family were enriched in both the mouse and human placenta.
392 This is consistent with the findings of others showing genes and proteins in the placenta overlap in the
393 two species^{14,15}. Indeed, as a key aim of our work was to create a secretome map that would be
394 applicable for both human and mouse, we used orthologue searches in our initial steps in narrowing

395 our list of protein candidates. We found that the majority of the proteins we found in our mouse
396 placental endocrine cell protein lists were also expressed by the human placenta, which is higher than
397 reported previously for other placental datasets. However, of note, we found that there were an
398 additional 31 secreted proteins in our complete placental secretome map, which were only expressed
399 by the mouse and not the human placenta. These included 17 members of the PRL/PL gene family and
400 7 members of the cathepsin gene family, which have both undergone robust species-specific
401 expansion, particularly in rodents, and exhibit unique spatial expression patterns by endocrine
402 trophoblast lineages in mice^{29,30}. Overall, PRL/PL and cathepsin family members are thought to play
403 divergent roles in driving physiological changes in the mother during pregnancy, including modulation
404 of insulin production and action, vascular remodelling and immune system regulation. However,
405 further work is required to understand the significance of individual family members to determining
406 pregnancy outcome.

407

408 Using a collection of published datasets, we identified that around 30-40% of proteins in our placental
409 secretome map (319 proteins expressed by human and mouse placenta) were reported to be
410 aberrantly expressed by the human placenta in pregnancy complications. Moreover, we found 4
411 secreted placental proteins to be differentially expressed in the placenta of women who developed
412 PE, GDM, IUGR and SGA. This suggests that there may be common pathways related to the production
413 of specific placental hormones, which may underlie or be reflective of the development of such
414 pregnancy complications. Alternatively, the common expression of secreted placental proteins
415 between these four pregnancy complications may reflect that there is overlap between these
416 pregnancy complications, as PE often leads to IUGR or SGA and GDM is linked to PE. Interestingly, two
417 of these proteins; FLT1 and IGF2 were highly enriched in the human placenta compared to other
418 tissues. Moreover, circulating FLT1 (sFLT1) has been previously reported as a suitable biomarker for
419 PE, IUGR and SGA. Whilst the expression of the FLT1 gene is reported to be altered in the placenta of
420 women with GDM, previous work has not evaluated whether sFLT1 levels are altered and could serve
421 as a biomarker for GDM pregnancies. Similarly, IGF2 was also reported to be altered in the placenta
422 in PE, IUGR, GDM and SGA pregnancies however, less is known about changes in circulating IGF2 in
423 the mother³¹⁻³⁶. Aside from being altered in LGA pregnancies, ANGPT2 and TIMP3 in our secretome
424 map were also reported to be differentially expressed by the placenta in the pregnancy complications
425 assessed. ANGPT2 has previously been explored as predictive candidate biomarker for PE, however it
426 was shown to be unsuccessful³⁷. In the context of GDM, ANGPT2 has been reported to be differentially
427 secreted from cultured trophoblast of the term placenta in GDM pregnancy³⁸, but no maternal serum

428 analysis was described. Similarly, altered placental expression of ANGPT2 were reported for SGA³⁹ and
429 one study has found it to serve as a predictive biomarker for IUGR⁴⁰.

430

431 We identified several secreted placental proteins altered specifically in some of the pregnancy
432 complications we studied. Analysing the gene ontology terms of these unique groups of proteins
433 revealed that for those uniquely altered in PE, they were implicated in the control of immune
434 processes, platelet aggregation and leukocytes like neutrophils, which is in line with previous work
435 focussed on understanding the pathogenesis of PE in women⁴¹. Similarly, GO analysis of the secreted
436 placental proteins specifically altered in GDM featured terms including protein metabolism,
437 extracellular matrix remodelling and the control of the unfolded protein response and is consistent
438 with studies exploring the aetiology of GDM⁴². Secreted placental proteins changed in IUGR are
439 proposed to be involved in fibrin, collagen and laminin interactions, however the functional relevance
440 of this finding requires further study.

441

442 As a proof of concept that our methodology and placental secretome map may be beneficial for
443 illuminating potential circulating biomarkers with clinical relevance, four secreted placental protein
444 (sFLT1, MIF, ANGPT2 and IGF2) were assessed in the serum of women who had normal or GDM
445 pregnancies. All four proteins were detectable as early as 12 weeks of gestation. We found that across
446 the two gestational time-points, sFLT1 was overall higher in the circulation of women who developed
447 GDM. This was despite the fact that the women with GDM were normotensive. Studies previously
448 exploring changes in sFLT1 in GDM pregnancies have yielded inconsistent results. There was no
449 difference in circulating sFLT1 concentration in lean women with and without GDM in the third
450 trimester of pregnancy⁴³, and no difference in the secretion of sFLT1 by term placental explant from
451 women who developed GDM⁴⁴. However, sFLT1 has been reported to be elevated in the early second
452 trimester (16-20 weeks of gestation) in women who went on to develop GDM in later pregnancy⁴⁵,
453 which is in line with our findings. The relationship between placental sFLT1 production and the
454 development of GDM warrants further study.

455

456 We found that the circulating levels of ANGPT2 and IGF2 were not different between women with
457 normal glucose tolerance or GDM at either 12 or 28 weeks of gestation. However, circulating levels of
458 MIF in the mother failed to decline in women with GDM between these two gestational time points.
459 Moreover, the ratios / relationships between the concentrations of MIF to sFLT1 and ANGPT2 to MIF

460 were altered in women at week 12 of pregnancy, which is at least 10 weeks before diagnosis of GDM,
461 suggesting that they may serve as potential early biomarkers for GDM. MIF promotes the secretion of
462 insulin from beta cells and also increases glucose uptake by skeletal muscle⁴⁶, thus its significance in
463 development of GDM should be explored further. The value of assessing the ratio / relationship
464 between the concentration of different biomarkers in the maternal circulation for early detection of
465 pregnancy complications is supported by previous work showing a change in the ratio of sFLT1 to PIGF
466 for PE, as well as IUGR in women^{2,47}. The number of women with normal glucose tolerance and GDM
467 in our study was small and both groups had an elevated body mass index. Further work is required to
468 validate our findings of a change in the ratios / relationships between MIF to sFLT1 and ANGPT2
469 concentrations in larger cohorts and in women who have a normal body mass index. Moreover, work
470 is required to further explore the clinical value of generating a secretome map of the placenta utilising
471 our approach.

472

473 We identified 33 transcription factors that are expressed by the STB of the human placenta and are
474 predicted to control the gene expression of approximately 30% of the proteins in our placental
475 secretome map (and are also expressed by the STB at the same time). Of these, ten were previously
476 linked with pregnancy complications. These included ARNT2, which is dysregulated in the placenta of
477 women with PE and IUGR and modulates the expression of genes that are also reported to be altered
478 in human pregnancy complications, such as ANGPT2¹². ARNT2 is implicated in mediating cellular
479 responses to stimuli including hypoxia⁴⁸ and our findings are consistent with recent work applying an
480 integrated systems biology approach⁴⁹. We also identified transcription factors, PLAG1 and CREB1 that
481 were altered in the placenta of GDM pregnancies and were predicted to modulate the expression of
482 numerous proteins in our secretome map including those that were additionally differentially
483 expressed in GDM, such as IGF2 and FLT1. Consistent with this, CREB1 is regulated by metabolic stimuli
484 like glucose⁵⁰ and PLAG1 was pinpointed as a critical factor altered in women who developed a
485 complicated pregnancy⁵¹. In addition, both PLAG1 and CREB1 have been reported to be dysregulated
486 in mouse genetic models showing placental dysfunction and/or poor pregnancy outcome^{52,53}. Thus,
487 numerous transcription factors likely govern the endocrine function of the placenta and may have
488 significance for understanding the pathogenesis of human pregnancy complications. Hence, future
489 work should centre on testing the significance and upstream regulators of transcription factors
490 identified as putative regulators of placental hormone production.

491

492 In summary, we have generated a comprehensive secretome map of the placenta. This map was
493 proven to be suitable for gaining further information on the significance and regulation of placental
494 endocrine function in mice and humans. Furthermore, we have uncovered different types of secreted
495 placental proteins, which function in the endocrine and paracrine regulation of maternal physiology,
496 but also possibly in an autocrine manner to modulate placental biology. Whether secreted placental
497 proteins may reach the fetal circulation to modulate fetal growth requires further exploration.
498 However, our placental secretome map revealed that more than 100 proteins may be differentially
499 secreted from the placenta in complicated human pregnancies. Further work is required to extend our
500 findings, including by employing the same methodology and bioinformatics pipeline however, using
501 placental endocrine cells taken from other gestational ages and pregnant mice exposed to
502 environmental conditions, such as maternal obesity, which is a risk factor for complications like PE,
503 GDM and abnormal birthweight. This will further build knowledge on the role and control of the
504 endocrine placenta during pregnancy and may pave the way for the discovery of novel or improved
505 biomarkers for early detection and prevention of pregnancy complications.

506

507 **Methods:**

508 **Animals**

509 All experiments were performed under the UK Home Office Animals (Scientific Procedures) Act 1986.
510 All mice used (wild type and transgenic) were on a C57BL/6 genetic background and housed under
511 12h dark-light conditions with free access to water and the standard diet (RM3, special dietary
512 services) used in the University of Cambridge Animal Facility. For the preparation of primary cultures
513 of junctional zone trophoblast endocrine cells, wild type females were mated with males homozygous
514 for *Tpbpa*-Cre-EGFP transgene¹³. For the fluorescence-activated cell sorting of junctional zone
515 trophoblast endocrine cells, *Tpbpa*-Cre-EGFP homozygote males were mated to females homozygous
516 for the double fluorescent Cre reporter construct, mTmG, which expresses membrane-targeted
517 tdTomato prior to, and membrane-targeted EGFP following, Cre-mediated excision (kind gift from Dr
518 Marika Charalambous, King's College London¹⁶). The day a copulatory plug was found was denoted as
519 day 1 of pregnancy (term is 20.5 days). Placentas were harvested from mouse dams that were
520 schedule 1 killed by cervical dislocation on day 16 of pregnancy.

521

522 **Preparation of primary cultures of junctional zone trophoblast endocrine cells**

523 Placentas (average of 6-8 per mouse dam) were enzymatically dissociated using a buffer (Medium 199
524 with Hank's salts, 20mM HEPES, 10mM NaHCO₃, 50U penicillin/ml, and 50pg streptomycin/ml, pH 7.4)
525 containing 0.1% collagenase and 0.002% DNase at 37°C for 1h, as described previously²⁰. Dissociated
526 samples were passed through a 200µM nylon filter to remove tissue debris and cells were centrifuged
527 at 500g for 5 minutes. Cell pellets were resuspended with Medium 199 X1 and cells subsequently
528 separated using a three layer Percoll density gradient (1.028, 1.05 and 1.088 g/ml) according to
529 manufacturer instructions (Percoll plus, GE Healthcare Life Sciences) and as described previously by
530 centrifuging at 600g for 30 minutes with controlled acceleration and braking. Layers from the density
531 gradient were recovered into medium199 X1 to dissolve the Percoll solution. Cells were then
532 centrifuged for 5 minutes at 500g and further washed with PBSX1 prior to counting using
533 Haemocytometer. Cells isolated from each layer of the Percoll gradient were fixed with 4% PFA for 20
534 min and subjected to 5µ/ml of Hoechst solution for 10 min at 37°C. Cells were then visualised using
535 fluorescence microscopy (Leica TCS SP8 Confocal laser scanning microscope) and the second layer was
536 found to contain the greatest density of junctional zone trophoblast endocrine cells (EGFP positive
537 cells due to Tpbpa-Cre-EGFP) and therefore used for further analysis. Namely, cells in the second
538 Percoll density layer were seeded in 96 well plates, 8 chamber-slides or in 6 well plates (10⁵ cells/ml)
539 and time of seeding was defined as time 0. Cells were grown in NTCT-135 medium containing 10%
540 fetal bovine serum, 50 IU/ml ampicillin, 50 µg/ml streptomycin, 2mM l-glutamine, 20 mM HEPES and
541 10 mM NaHCO₃ and maintained in a humidified atmosphere of 5% CO₂ at 37°C. Cell medium was
542 replaced every 24h. Cells were washed three times in PBSX1 and serum-free medium applied 24h prior
543 to any downstream analysis.

544

545 **Viability assay**

546 Cell viability was determined using an XTT cell proliferation assay kit (Abcam- ab232856) according to
547 manufacturer's instructions. Values were calculated as % of values at time 0h and each experiment
548 was performed in triplicate in 8-10 independent assays.

549

550 **Cell death assay (LDH release assay)**

551 Cell death was determined by measuring the activity of lactate dehydrogenase (LDH) in the
552 conditioned media of primary cell cultures using a LDH cytotoxicity assay kit, according to the
553 manufacturer's instructions (Thermo scientific). Cell-free medium and cells treated with medium

554 containing Triton-X were used as negative and positive controls, respectively. Each experiment was
555 performed in triplicate in 6 independent assays.

556

557 **In situ hybridisation**

558 In situ hybridization was performed on primary cell cultures seeded on chamber slides at 90%
559 confluency (10^6 cells/well) (Thermofisher Scientific, UK). Cells were fixed in 4% PFA for 30 min, washed
560 twice with PBSX1, dehydrated in increasing concentrations of ethanol and stored in 100% ethanol at -
561 20°C. In situ hybridization was performed using the RNAScope 2.5 RED chromogenic assay kit following
562 the manufacturer's instructions (Bio-Techne, UK). Briefly, slides were allowed to equilibrate to room
563 temperature and rehydrated in PBSX1. RNAscope® Hydrogen Peroxide was applied to the slides for 10
564 min at RT, followed by RNAscope® Protease Plus in RT for 10 min. Slides were then incubated with the
565 target or control probes at 40°C for 2h (negative control probe (310043), positive control probe
566 (313911), Tpbpa-probe (405511), Prl8a8-probe (528641), Gjb3-probe (508841) and Hand1-probe
567 (429651) in a HybEZ oven for 2h at 40°C. Next, slides were washed twice with wash buffer and were
568 subjected to 6 rounds of amplification and the probe signal was developed via a reaction with fast red.
569 Slides were then counterstained with Haematoxylin and mounted in EcoMount. Slides were scanned
570 on a NanoZoomer 2.0-RS slide scanner (Hamamatsu, Hamamatsu City, JP) at 40x magnification.

571

572 **Conditioned medium preparation for mass spectrometry**

573 Conditioned medium from cultured cells was collected at 48h of culture. At 24h prior to medium
574 collection, cells were washed three times with PSBX1 and cultured in serum-free medium. The
575 conditioned medium was centrifuged at 1000g for 10 min and total protein concentration measured
576 using a Bradford assay. Proteins in the conditioned medium were concentrated up to 1.2ug/ul of total
577 protein using cellulose membrane Ultra-4 Centrifugal Filter Unit of 3KDa cut-off (Merck) as per the
578 manufacturer instructions.

579

580 **RNA extraction and quantitative real time PCR (qPCR)**

581 Total RNA was extracted from cultured cells using RNeasy Plus Mini Kit (QIAGEN) and 0.5 µg of RNA
582 was reverse transcribed with random hexamer primers using a High-Capacity cDNA RT kit (Applied
583 Biosystems) according to the manufacturer's instructions. qPCR was performed using MESA BLUE
584 qPCR Master Mix (Eurogentec) on a Bio-Rad T100 thermocycler using gene-specific intron-flanking

585 primers. Gene expression was analysed in triplicate and the Ct values were normalised to the
586 expression of internal housekeeping genes (*Gapdh*, *Rpl11* and *Hprt*). Results are presented as mean \pm
587 SEM and relative to time 0h.

588

589 **Fluorescence-activated cell sorting (FACS) of live cells for mass spectrometry**

590 Single cell suspensions were prepared from whole placentas digested with the dissociation buffer
591 containing 0.1% collagenase and 0.002% DNase at 37°C for 1h, as described for the preparation of
592 primary cell cultures. Cells were filtered through 100 μ M nylon filter and centrifuged at 500g for 5
593 minutes. Cell pellets were resuspended with PBSX1 and 7AAD (Life Technologies, A1310) added prior
594 sorting using a FACSJazz machine (BD Biosciences, Singapore). Live cells were gated and cells positive
595 for EGFP or tdTomato were sorted and lysed directly into 80% acetonitrile (ACN) in water (v/v) in a
596 Protein LoBind Eppendorf tube.

597

598 **Mass spectrometry**

599 **LC-MS/MS analysis of conditioned media**

600 Conditioned media from primary cultures of trophoblast cells were standardised to a final
601 concentration of 2 μ g/ μ l in 4% SDS loading buffer with 100mM dithiothreitol (DTT). Samples were
602 denatured at 95°C for 5 min and 10 μ g of total protein per sample was loaded onto a 12% SDS PAGE
603 gel and run at 120 Volts. The gel was then stained with colloidal coomassie stain and washed with
604 water. Protein bands in each lane were cut into 1mm² pieces, de-stained, reduced (using DTT) and
605 alkylated (using iodoacetamide) and subjected to enzymatic digestion with sequencing grade Trypsin
606 (Promega, Madison, WI, USA) overnight at 37°C. After digestion, the supernatant was pipetted into a
607 sample vial and loaded onto an autosampler for automated LC-MS/MS analysis. All LC-MS/MS
608 experiments were performed using a Dionex Ultimate 3000 RSLC nanoUPLC (Thermo Fisher Scientific
609 Inc, Waltham, MA, USA) system and a Q Exactive Orbitrap mass spectrometer (Thermo Fisher Scientific
610 Inc, Waltham, MA, USA) as described previously.

611

612 For medium generated spectra, all MS/MS data were converted to mgf files and the files were then
613 submitted to the Mascot search algorithm (Matrix Science, London UK, version 2.6.0) and searched
614 against the UniProt mouse database (61295 sequences; 27622875 residues) and a common
615 contaminant sequences containing non-specific proteins such as keratins and trypsin (115 sequences,

616 38274 residues). Variable modifications of oxidation (M) and deamidation (NQ) were applied, as well
617 as a fixed modification of carbamidomethyl (C). The peptide and fragment mass tolerances were set
618 to 20ppm and 0.1 Da, respectively. A significance threshold value of $p < 0.05$ and a peptide cut-off score
619 of 20 were also applied. All data (DAT files) were then imported into the Scaffold program (Version
620 4.5.4, Proteome Software Inc, Portland, OR).

621

622 **LC-MS/MS analysis of primary cultured cells and sorted cells**

623 Trophoblast from both primary cell cultures and fluorescence activating cell sorting were treated with
624 800 μ L of 80% ACN in water and centrifuged for 5 min at 10,000g. The supernatant was removed and
625 the pellet was reduced and alkylated using 50mM ammonium bicarbonate and 10mM DTT at 60°C for
626 1h, followed by the addition of 100mM iodoacetamide in the dark for 30min. Enzymatic digestion was
627 performed using Trypsin at 10 μ g/mL in 50mM ammonium bicarbonate overnight at 37°C (enzymatic
628 digestion was halted by the addition of 1% formic acid). Samples were analysed by LC-MS using a
629 Thermo Fisher Ultimate 3000 nano LC system coupled to a Q Exactive Plus Orbitrap mass spectrometer
630 (ThermoScientific, San Jose, CA, USA) as described previously. For generated spectra, all LC-MS files
631 were searched using PEAKS 8.5 (Bioinformatics Solutions Inc) software against the Swissprot database
632 (downloaded 26-Oct-2017) with a *Mus musculus* filter. For the proteins, a tryptic digestion approach
633 was used with a semi-specific setting and up to a maximum of 3 missed cleavages. The search outputs
634 had a 1% FDR setting applied, along with a unique peptide setting of at least 1 peptide. The precursor
635 and product ion tolerances were 10 ppm and 0.05 Da, respectively.

636

637 **Bioinformatics analysis**

638 Protein/peptide annotations in LC-MS datasets were converted to their gene accession ID via UniProt
639 (<https://www.uniprot.org/uploadlists/>). Gene lists were then overlaid with publicly available datasets
640 for the mouse and human placenta, which are detailed in Supplementary Table 1 (3 from mouse
641 placenta and 8 for human placenta). Mouse-human ortholog searches were also undertaken using
642 three sources of data, MGI (<http://www.informatics.jax.org/>), NCBI
643 (<https://www.ncbi.nlm.nih.gov/homologene>) and Ensembl (biomaRt_2.42.1 and homologene_1.4.68
644 in R version 3.6.2; <https://www.R-project.org/>). Then using R, a combined ortholog list for Mouse-
645 Human was generated (details of the list and Rscript can be found in GitHub, <https://github.com/CTR->
646 [BFX/2020-Napso_Sferruzzi-Perri](https://github.com/CTR-BFX/2020-Napso_Sferruzzi-Perri)). Mouse-human ortholog results were classified as one-to-one when
647 a gene/protein from mouse was found at the end of a node in human. Any results classified as one-

648 to-many were excluded. Gene ontology analyses were performed using both STRING and Panther
649 tools (<https://string-db.org/>). Gene enrichment analyses were conducted using TissueEnrich
650 (<https://tissueenrich.gdcb.iastate.edu/>), which utilises datasets available in the Human Protein Atlas
651 compiling RNAseq datasets from 35 human tissues and the Mouse ENCODE database comprised of
652 RNAseq datasets of 17 mouse tissues. Refined gene/protein lists were overlaid with publicly available
653 RNA and protein expression datasets for human pregnancy complications (Supplementary Table 2)
654 and aided by searches in Pubmed and the OMIM repository (<http://www.ncbi.nlm.nih.gov>).

655

656 To further refine our lists to secreted proteins, we applied SignalP (Signal Peptide Prediction, version
657 4.1; ⁵⁴) and gene ontology analysis using four different gene ontology (GO) terms: extracellular region
658 (GO: 0005615), extracellular exosome (GO: 0070062), extracellular region parts (GO: 0005615) and
659 signal IP (excluding signals detected for ER lumen proteins)⁵⁵. This was undertaken because SignalP
660 can only detect the signal peptide for proteins secreted via the canonical route, which is also known
661 as the "classic" or "conventional" secretion pathway. However, eukaryotic cells also utilize an
662 unconventional protein secretion route for protein sorting and delivery, an "unconventional"
663 secretion pathway, including leaderless proteins that are secreted into the extracellular space. This
664 approach allowed us to capture proteins that employ the "conventional", as well as "unconventional"
665 secretion pathways. All data outputs at each step of the pipeline, including the proteins/genes
666 expressed in the mouse but not the human placenta and the refinement of our list to secreted proteins
667 can be found in GitHub (https://github.com/CTR-BFX/2020-Napso_Sferruzi-Perri).

668

669 To search for enrichment of transcription factor (TF) binding motifs at the promoters of the genes
670 encoding the 319 proteins that are part of placental secretome, we first used EPD (Eukaryotic
671 Promoter Database - <https://epd.vital-it.ch/index.php>) to retrieve the DNA sequences from 1,000bp
672 upstream to 100bp downstream of the transcriptional start site (TSS). These sequences were then
673 analysed using AME (Analysis of Motif Enrichment v4.12.0 - <http://meme-suite.org/tools/ame>) by
674 selecting *Mus musculus* and HOCOMOCO Mouse (v11 FULL) as motif database. An additional search
675 for upstream regulators was performed using the Ingenuity Pathway Analysis (IPA, Qiagen), and only
676 TFs predicted by both tools (n=77) were selected for further analysis. Next, we filtered for TFs with
677 enriched expression in STB cells from human placenta at 8 weeks of gestation that had at least one
678 common target gene encoding one of the 319 placental secretome proteins (n=33). Literature search
679 led to identification of ten of those TFs that were linked with pregnancy complications. Transcriptional
680 network visualization for the 10 TFs and the corresponding targets was performed using IPA.

681

682 **Human study population and sampling**

683 Peripheral blood samples were retrospectively selected for this study from women recruited via the
684 Ophelia study (REC number 18/LO/0477 approved 5/4/2018). Inclusion criteria included (1) singleton
685 pregnancy, (2) no evidence of severe congenital anomaly and (3) a referral for an oral glucose
686 tolerance test (OGTT) for clinical reasons, according to NICE guidelines
687 (<https://www.nice.org.uk/guidance/ng3>). Exclusion criteria for this study were (1) multiple pregnancy
688 (2) severe congenital anomaly on ultrasound, (3) severe anaemia on previous blood tests, (4) previous
689 diagnosis of diabetes outside of pregnancy and (5) medications at the time of the OGTT, which may
690 interfere with the results of the OGTT. Screening for GDM was performed at 24 weeks of gestation
691 using a 75 g OGTT and diagnosis of GDM was made in accordance with the IADPSG glycaemic cut-off
692 values (fasting value ≥ 92 mg/dL (5.1 mmol/L), 1 h post-glucose load ≥ 180 mg/dL (10 mmol/L), 2 h
693 post-glucose load ≥ 153 mg/dL (8.5 mmol/L). Blood samples were collected from pregnant women in
694 the 1st trimester (12 weeks of gestation) and 2nd trimester (28 weeks of gestation) and were analysed
695 for HbA1c concentration. Plasma was recovered by 2500 rpm for 10min and samples were stored at -
696 80c. Blood pressure measurements were taken at various times in pregnancy using a calibrated
697 automatic oscillometric sphygmomanometer (Dinamap, machine) and systolic and diastolic blood
698 pressure recorded. For inclusion in this study, women with GDM were selected and a control group of
699 age- and BMI-matched participants with normal glucose tolerance were included for comparison.
700 Further details about the OPHELIA study are provided elsewhere (Research Registry number 5528)⁵⁶.

701

702 **Human plasma analysis of protein candidates by ELISA**

703 Candidate secreted placental proteins were quantified in maternal plasma samples from healthy
704 women and those diagnosed with GDM, using commercially available ELISAs for sFLT1 (K15190D,
705 MSD), MIF (K151XJK-1, MSD), ANGPT2 (F21YR-3, MSD) and IGF2 (DG200, R&D) by the Core
706 Biochemical Assay Laboratory, Cambridge and according to the manufacturer's instructions.

707

708 **Statistical analysis**

709 Data for viability, cell death and qRT-PCR are presented as mean \pm SEM. Two-way ANOVAs (with Tukey
710 correction for multiple comparisons) or t-tests were used for determining significant differences. All

711 analyses were performed using GraphPad Prism version 7.00 (GraphPad Software). $P < 0.05$ was
712 considered to indicate a statistically significant difference between the groups analysed.

713

714 **Funding**

715 This work was supported by a Royal Society Dorothy Hodgkin Research Fellowship, Academy of
716 Medical of Sciences Springboard Grant, Isaac Newton Trust Grant and Lister Institute Research Prize
717 grant to ANSP (grant numbers DH130036 / RG74249, SBF002/1028 / RG88501, RG97390 and
718 RG93692, respectively). TN was supported by an EU Marie Skłodowska-Curie Fellowship
719 (PlaEndo/703160) and an Early Career Grant from the Society for Endocrinology. CLM is supported by
720 the Diabetes UK Harry Keen Intermediate Clinical Fellowship (DUK-HKF 17/0005712) and the EFSD-
721 Novo Nordisk Foundation Future Leader's Award (NNF19SA058974). Work in the FR/FMG laboratory
722 was supported by the Wellcome Trust (106262/Z/14/Z,106263/Z/14/Z), the MRC
723 (MRC_MC_UU_12012/3 and MRC -Enhancing UK clinical research grant MR/M009041/1) and the
724 Cambridge Biomedical Research Centre (NIHR-BRC Gastrointestinal Diseases theme).

725

726

727 **Acknowledgements**

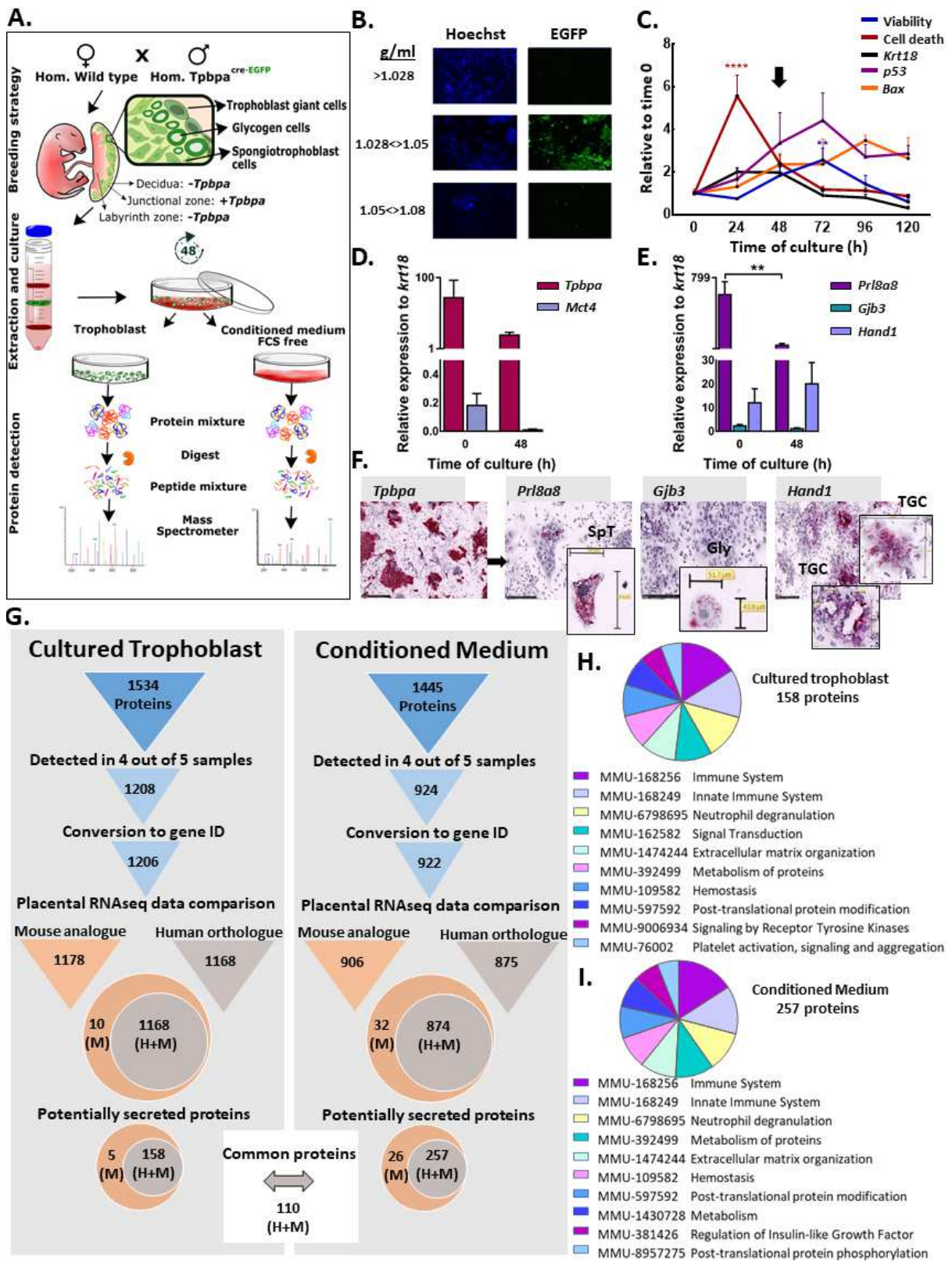
728 We would like to thank Dr Marika Charalambous, King's College London for the mTmG mouse line. We
729 would like to thank the staff in Combined Animal Facility, as well as Dr. Jorge Lopez-Tello and Miss
730 Bethany R.L. Aykroyd, Centre for Trophoblast Research, Department of Physiology, Development and
731 Neuroscience, University of Cambridge for their assistance in the breeding and husbandry of mice. We
732 would like to thank Dr. Laura Kusinski, Wellcome-MRC Institute of Metabolic Science, Addenbrooke's
733 Hospital, Cambridge for locating the samples from pregnant women who volunteered to participate
734 in the Ophelia study. Finally, we thank the Bioinformatics and Biostatistics (Bio2) Core Facility of the
735 Wellcome-MRC IMS-MRL for the support provided by facilitating the access to data analysis tools.

736

737 **Conflict of Interest**

738 Authors do not have any competing financial interests in relation to the work described.

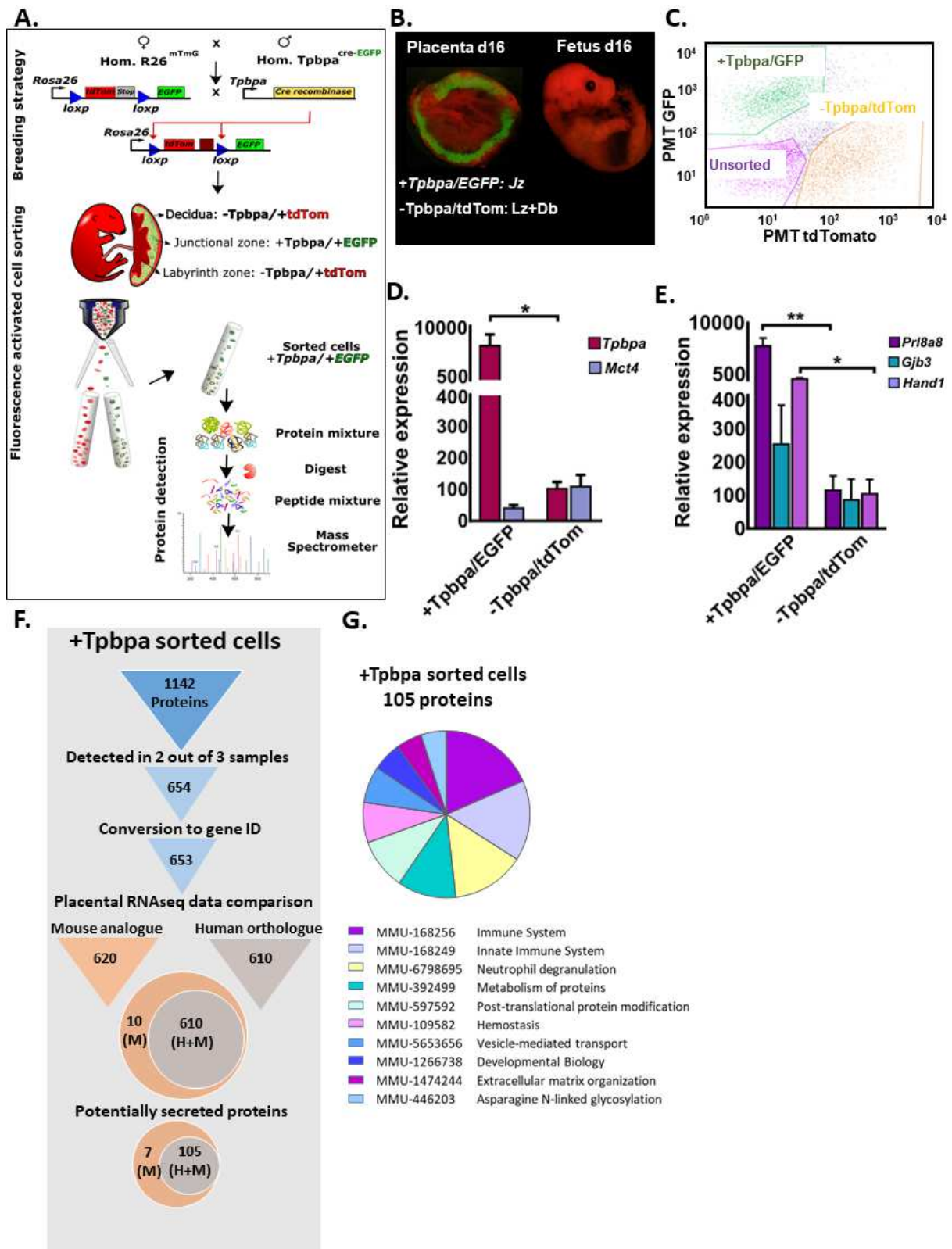
739



741

742 Figure 1: Detection of secreted proteins in primary cultures of mouse trophoblast.

743 **A)** Workflow for the detection of secreted proteins in primary cultures of trophoblast from mice at
744 day 16 of pregnancy. **B)** Visualisation of EGFP (*Tpbpa*-Cre-EGFP reporter) by fluorescence microscopy
745 to identify the Percoll gradient layer containing trophoblast endocrine cells. Cells in layers were
746 counterstained with Hoechst dye (blue) and photographed at magnification 10X (scale bar-0.6mm). **C)**
747 Primary cell culture viability (determined by XTT), cell death (LDH release levels), trophoblast density
748 (*Krt18* gene expression) and apoptosis (*p53* and *Bax* gene expression) from time 0 to 120h. **D)**
749 Proportion of junctional zone (*Tpbpa* gene expression) and labyrinthine zone (*Mct4* gene expression)
750 trophoblast at 0h and 48h. **E)** Relative abundance of the three junctional zone endocrine cell types,
751 spongiotrophoblast, glycogen cells and giant cells (gene expression of *Prl8a8*, *Gjb3* and *Hand1*,
752 respectively) at 0h and 48h of culture. **F)** Representative images of cells stained in situ using RNAscope
753 probes against; *Tpbpa*, *Prl8a8*, *Gjb3* and *Hand1* to visualise trophoblast endocrine cells,
754 spongiotrophoblast (SpT), glycogen cells (Gly) and giant cells (TGC), respectively. **G)** Pipeline and
755 results of the analysis of proteins detected by mass spectrometry in cultured trophoblast and their
756 conditioned medium including conversion to RNA sequences and overlay with published RNA data for
757 the mouse and human placenta. Secreted proteins identified using SignalP and combined gene
758 ontology (GO) terms: extracellular region, extracellular exosome, extracellular region parts and signal
759 IP. **H and I)** Pathway over-representation analysis using Reactome pathway by STRING V.11 for the
760 158 and 257 secreted placental proteins in cultured trophoblast and their conditioned medium,
761 respectively that are expressed by both mouse and human placenta. XTT, LDH and gene expression
762 data relative to geometric mean of three housekeeping genes: *Gapdh*, *RPII* and *Hprt* are presented as
763 mean \pm SEM and expressed relative to expression at time 0h. Asterisks denote statistical significance
764 versus time 0h, using Two-way ANOVA (B) or t-test (C-D), **P<0.01, ****P<0.001, n=6-10 of 4 pooled
765 litters.



766

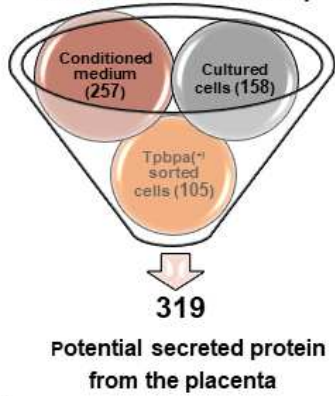
767 **Figure 2. Detection of secreted proteins in sorted mouse trophoblast endocrine cells.**

768 **A)** Workflow for the cell sorting and protein expression analysis of mouse trophoblast endocrine cells

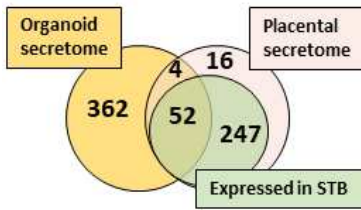
769 from mice at day 16 of pregnancy. **B)** Fluorescent image of placenta showing EGFP in *Tpbpa* positive

770 cells (junctional zone of the placenta) and tdTom for *Tpbpa* negative cells. **C)** Representative image of
771 cell sorting of EGFP/tdTom cells by fluorescence activated cell sorting. **D)** Expression of junctional zone
772 and labyrinth zone markers, *Tpbpa* and *Mct4*, respectively in the EGFP and TdTom sorted cells. **E)**
773 Expression of markers for junctional zone cell types, spongiotrophoblast cell (*Prl8a8*), glycogen cells
774 (*Gjb3*) and giant cells (*Hand1*). **F)** Pipeline and results of the analysis of proteins detected by mass
775 spectrometry in sorted *Tpbpa*+/*EGFP* cells. **G)** Pathway over-representation analysis using Reactome
776 pathway by STRING V.11 for the 105 secreted placental proteins expressed by both mouse and human
777 placenta. Data presented as mean \pm SEM and genes expressed relative to geometric mean of two
778 housekeeping genes: *RPII* and *Hprt*. Asterisks denote statistical significance to the *Tpbpa*+/*EGFP* sorted
779 cells, using t-test, * $P < 0.05$, ** $P < 0.01$, $n = 5$ for each group.

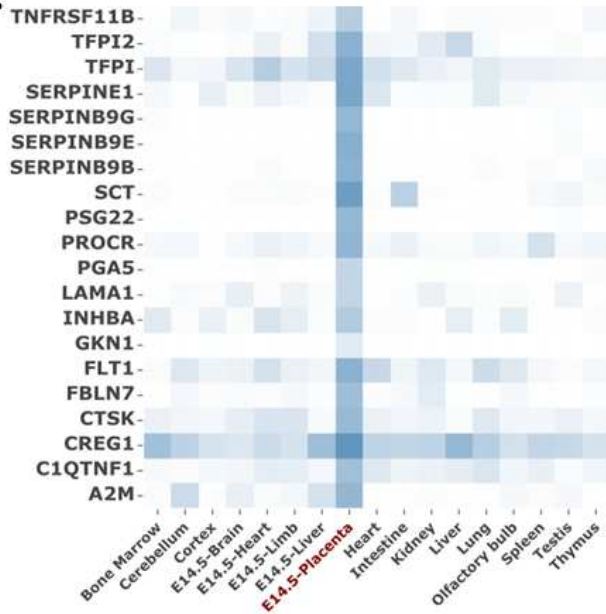
A. Placental secretome map



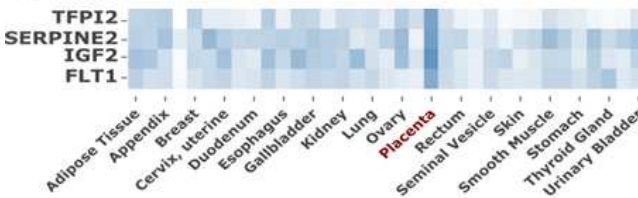
B.



D.



E.



C. Biological Process

#Term ID	Term description	# obs.	FDR
GO:0050896	Response to stimulus	204	2.44E-31
GO:0051239	Regulation of multicellular organismal process	128	1.46E-29
GO:0065008	Regulation of biological quality	138	3.54E-28
GO:0006950	Response to stress	126	5.19E-28
GO:0032501	Multicellular organismal process	181	6.5E-26
GO:0050793	Regulation of developmental process	110	5.53E-24
GO:0048519	Negative regulation of biological process	157	7.33E-24

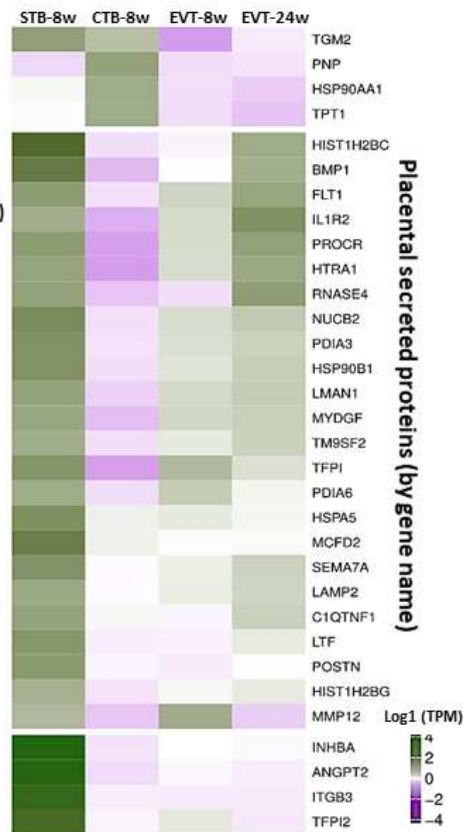
Molecular Function

#Term ID	Term description	# obs.	FDR
GO:0005515	Protein binding	199	9.02E-31
GO:0005488	Binding	258	5.2E-28
GO:0005102	Signaling receptor binding	85	1.31E-24
GO:0044877	Protein-containing complex binding	61	8.93E-17
GO:0005509	Calcium ion binding	44	6.79E-16
GO:0050840	Extracellular matrix binding	18	1.66E-15
GO:0002020	Protease binding	24	2.04E-15

Protein Domains

#Term ID	Term description	# obs.	FDR
IPR023795	Serpin, conserved site	13	3.04E-09
IPR000742	EGF-like domain	22	5.60E-09
IPR008160	Collagen triple helix repeat	14	7.34E-09
IPR000215	Serpin family	13	1.11E-08
IPR009030	Growth factor receptor cysteine	16	1.57E-08
IPR001464	Annexin	7	2.37E-07
IPR000867	Insulin-like growth factor-binding protein	7	3.88E-06

F.



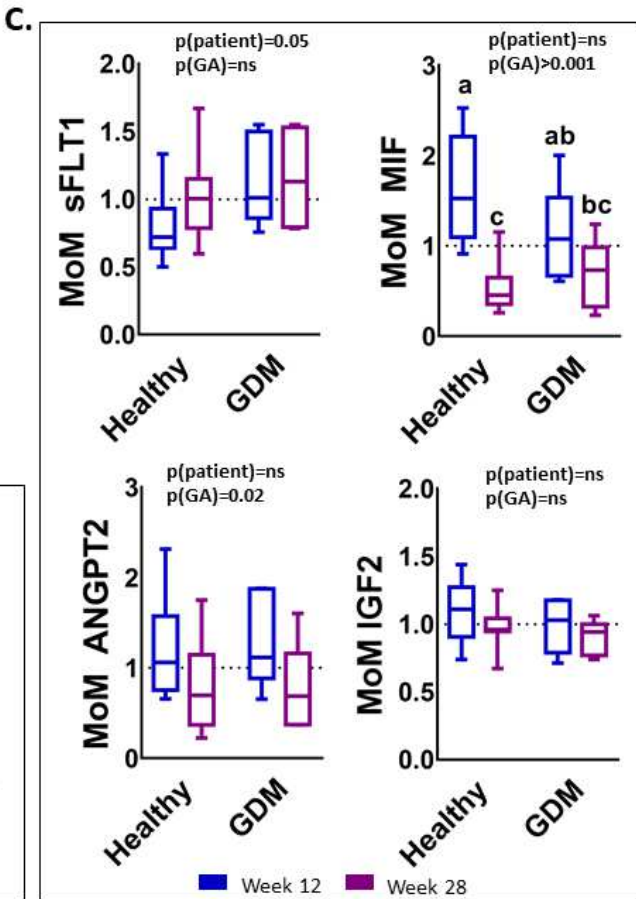
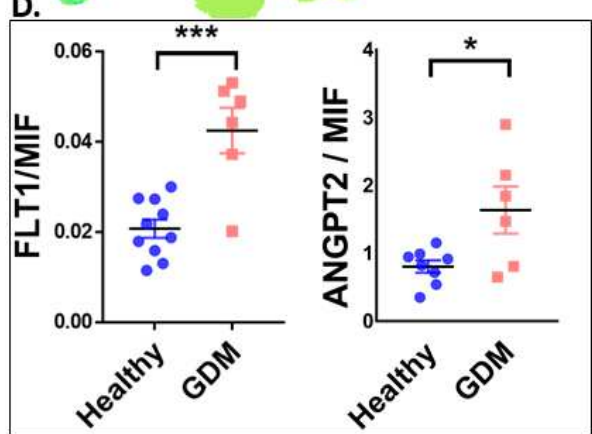
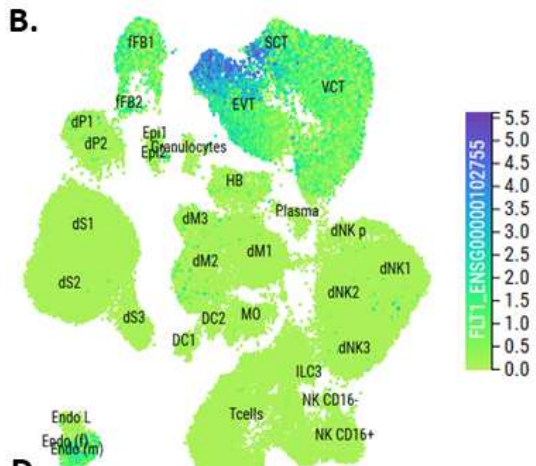
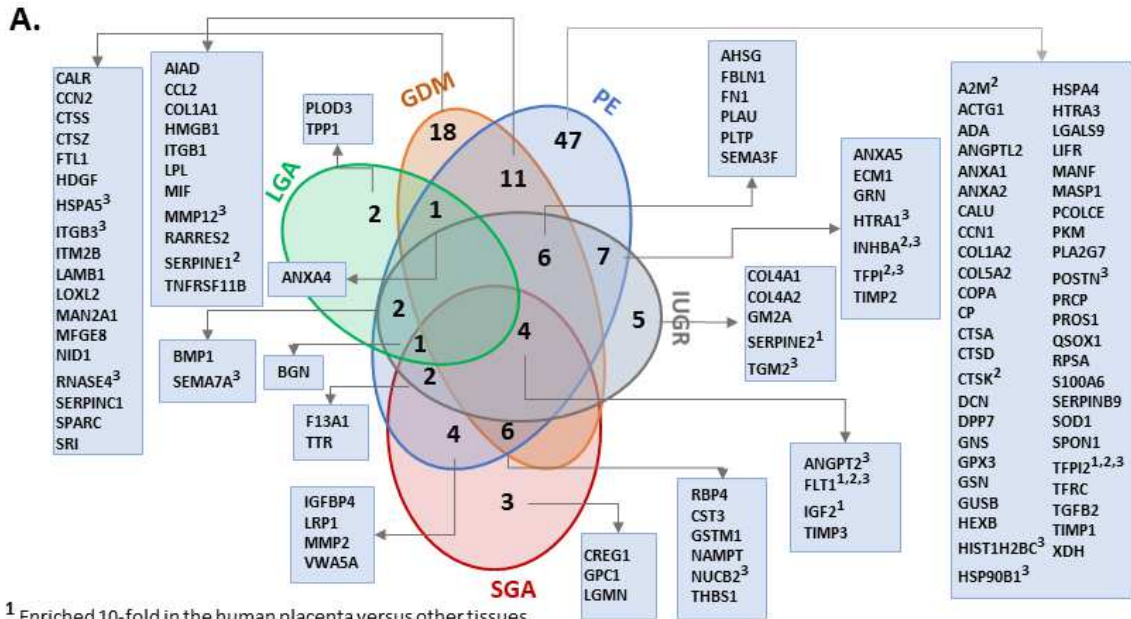
780

781 **Figure 3. Secretome map of the placenta**

782 **A)** Integrating the lists of secreted placental proteins expressed by mouse and human placenta and

783 obtained using our different methods to generate a comprehensive placental secretome map.

784 Proteins expressed by mouse but not human placenta shown in Supplementary data figure 1. **B)** Venn
785 diagram showing the overlay of placental secretome map with first trimester trophoblast organoid
786 secretome (Turco, 2018) and single cell RNAseq analysis for human placenta at 8 weeks of gestation
787 (Liu, 2018). **C)** Gene ontology (GO) analysis for the 319 secreted proteins detected in placental
788 secretome map using STRING V.11. **D and E)** Proteins in the placental secretome map that are highly
789 enriched in the placenta of mouse (**D**) and human (**E**) compared to other tissues using TissueEnrich. **F)**
790 Cell specific expression of the top 30 most highly expressed genes in the placental secretome map
791 using single cell RNAseq data for the human placenta (see results text for details). CTB:
792 cytotrophoblasts, STB: syncytiotrophoblast, EVT: extravillous trophoblasts, w: weeks.



793

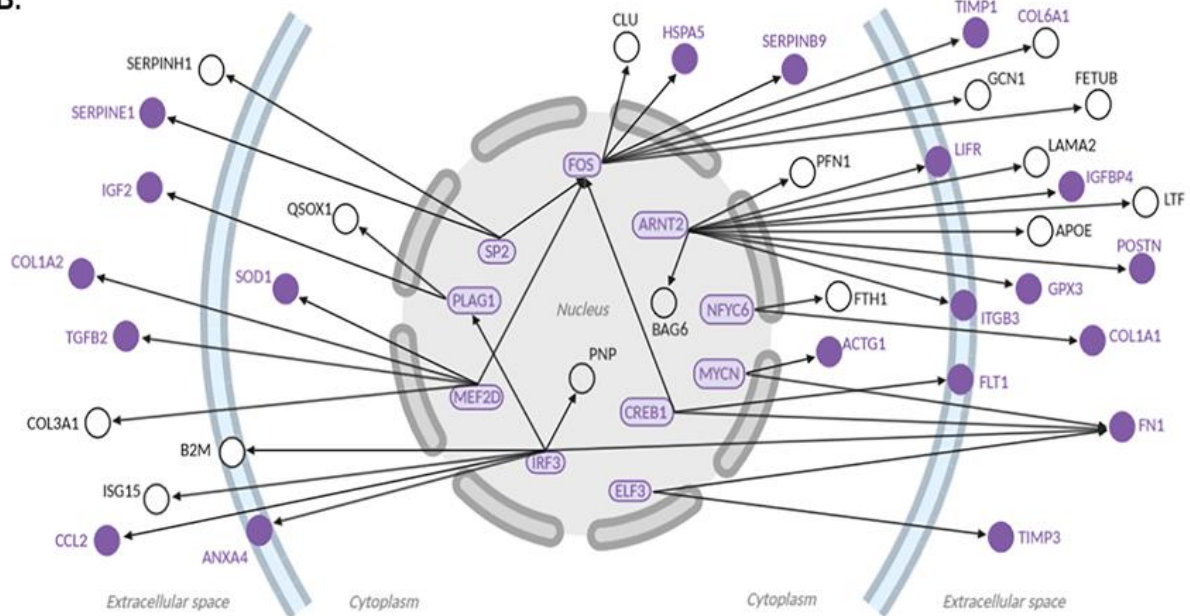
794 **Figure 4. Applying the secretome map of the placenta to data available for human pregnancy**
 795 **complications.**

796 **A)** Venn diagram showing the number of placental proteins in the secretome map that are
797 differentially expressed in the placenta of women with a pregnancy complication. **B)** FLT1 expression
798 at the maternal–fetal interface of early human pregnancy via the CellxGene tool ([https://maternal-](https://maternal-fetal-interface.cellgeni.sanger.ac.uk/)
799 [fetal-interface.cellgeni.sanger.ac.uk/](https://maternal-fetal-interface.cellgeni.sanger.ac.uk/)). **C)** Serum levels of FLT1, MIF, ANGP2 and IGF2 in pregnant
800 women at 12 and 28 weeks of gestation who went on to have normoglycemic (healthy) pregnancies
801 or developed GDM. Data are expressed as multiple for the median; MoM. **D)** Ratio of the levels of
802 FLT1 to MIF and ANGPT2 to MIF at week 12 of pregnancy in healthy women and those who went on
803 to develop GDM. Data are presented as mean \pm SEM of MoM. Raw data for proteins levels are shown
804 in supplementary figure 4. Asterisks denote statistical significance to the GDM pregnancies, using two
805 way-ANOVA for C and t-test for D, *P<0.05, **P<0.01, n=10-11 for healthy pregnancies, n=6 for GDM.
806 GDM: gestational diabetes mellitus, IUGR: intrauterine growth restriction, LGA: large for gestational
807 age, PE: preeclampsia, SGA small for gestational age.

A.

TF	Motif	IPA (p value)	AME (adjusted p value)	Common (DEG in pathology complications)	Complications (TF as DEG)	Reference
ARNT2		14/319 (1.71E-06)	174/319 (1.30E-13)	10 (5)	PE SGA	Leavey et al. 2015 Sober et al. 2015
ELF3		3/319 (1.04E-02)	161/319 (5.07E-08)	2 (2)	PE IUGR	Sober et al. 2015
PLAG1		3/319 (4.34E-02)	185/319 (1.82E-04)	2 (1)	GDM	Sober et al. 2015
SP2		2/319 (1.87E-02)	166/319 (2.45E-51)	2 (1)	IUGR LGA PE	Sober et al. 2015
MEF2D		6/319 (5.59E-04)	124/319 (3.84E-23)	4 (3)	IUGR PE	Sober et al. 2015
MYCN		25/319 (5.51E-13)	71/319 (1.40E-08)	2 (2)	PE	Leavey et al. 2015
FOS		49/319 (4.45E-24)	41/319 (1.37E-02)	7 (3)	PE	Gormley et al. 2017
NFYC		4/319 (2.93E-03)	38/319 (7.54E-10)	2 (1)	PE	Leavey et al. 2015
CREB1		22/319 (2.69E-05)	10/319 (1.83E-02)	2 (2)	GDM	Bari et al. 2016
IRF3		9/319 (8.50E-03)	162/319 (5.83E-54)	6 (3)	GDM PE	Sober et al. 2015 Leavey et al. 2015

B.



808

809 **Figure 5. Transcription factors dysregulated in pregnancy complications identified as possible**
 810 **regulators of genes encoding secreted placental proteins.**

811 **A)** Table showing the ten transcription factors with altered expression in pregnancy complications and
812 with binding sites enriched at the promoters of genes encoding proteins in the placental secretome
813 map. **B)** Regulatory network built with the ten transcription factors listed in panel A. The ten
814 transcription factors and their targets that are differentially expressed in pregnancy complications are
815 highlighted in purple. Location of the target proteins is according to their main cellular/extracellular
816 compartment indicated by IPA. The graph was generated using BioRender.

817

818 **Table 1: Clinical characteristics of women used for the analysis of circulating placental hormone**
819 **abundance in human pregnancy.**

Characteristics	Healthy pregnancy (n=10)	GDM pregnancy (n=6)	<i>p</i> (t-test)
Parity	1.14 ± 0.26	1.29 ± 0.52	0.78
Early pregnancy BMI	33.45 ± 1.78	35.37 ± 2.42	0.52
GA at OGTT	28.513 ± 0.75	26.55 ± 1.83	0.28
OGTT 0h (mmol/L)	4.46 ± 0.07	5.07 ± 0.2	0.002
OGTT 2h (mmol/L)	5.65 ± 0.23	7.66 ± 0.94	0.014
Systolic BP (mm Hg) 1 st trimester	116.8 ± 0.8	112.5 ± 1.8	0.386
Diastolic BP (mm Hg) 1 st trimester	71.09 ± 0.84	68.0 ± 2.1	0.576
Systolic BP (mm Hg) 2 nd trimester	117 ± 1.75	122.5 ± 4.26	0.541
Diastolic BP (mm Hg) 2 nd trimester	70.66 ± 1.6	71.75 ± 3.43	0.855
HBA1C (mmol/mol)	33.42 ± 0.58	36.0 ± 0.53	0.01
GA at delivery	39.47 ± 0.41	38.76 ± 0.57	0.30
Birthweight (g)	3556.36 ± 126.24	3392.1 ± 170.00	0.44

820 GA = gestational age, BP= Blood pressure

821

822 References

- 823 1 Napso, T., Yong, H. E. J., Lopez-Tello, J. & Sferruzzi-Perri, A. N. The Role of Placental Hormones
824 in Mediating Maternal Adaptations to Support Pregnancy and Lactation. *Front Physiol* **9**, 1091,
825 doi:10.3389/fphys.2018.01091 (2018).
- 826 2 Gaccioli, F., Aye, I., Sovio, U., Charnock-Jones, D. S. & Smith, G. C. S. Screening for fetal growth
827 restriction using fetal biometry combined with maternal biomarkers. *Am J Obstet Gynecol* **218**,
828 S725-S737, doi:10.1016/j.ajog.2017.12.002 (2018).
- 829 3 Zeisler, H. *et al.* Predictive Value of the sFlt-1:PIGF Ratio in Women with Suspected
830 Preeclampsia. *N Engl J Med* **374**, 13-22, doi:10.1056/NEJMoa1414838 (2016).
- 831 4 Amanda N.Sferruzzi-Perri, JorgeLopez-Tello, TinaNapso & E.J.Yong, H. Exploring the causes
832 and consequences of maternal metabolic maladaptations during pregnancy: Lessons from
833 animal models. *Placenta*, doi:10.1016/j.placenta.2020.01.015 (2020).
- 834 5 Bowen, J. M., Chamley, L., Mitchell, M. D. & Keelan, J. A. Cytokines of the placenta and extra-
835 placental membranes: biosynthesis, secretion and roles in establishment of pregnancy in
836 women. *Placenta* **23**, 239-256, doi:10.1053/plac.2001.0781 (2002).
- 837 6 Li, H. *et al.* LIFR increases the release of soluble endoglin via the upregulation of MMP14
838 expression in preeclampsia. *Reproduction* **155**, 297-306, doi:10.1530/REP-17-0732 (2018).
- 839 7 Lin, R. *et al.* Association of maternal and fetal LEPR common variants with maternal glycemic
840 traits during pregnancy. *Sci Rep* **7**, 3112, doi:10.1038/s41598-017-03518-x (2017).
- 841 8 Kaitu'u-Lino, T. J. *et al.* Circulating SPINT1 is a biomarker of pregnancies with poor placental
842 function and fetal growth restriction. *Nat Commun* **11**, 2411, doi:10.1038/s41467-020-16346-
843 x (2020).
- 844 9 Armstrong, D. L. *et al.* The core transcriptome of mammalian placentas and the divergence of
845 expression with placental shape. *Placenta* **57**, 71-78, doi:10.1016/j.placenta.2017.04.015
846 (2017).
- 847 10 Knox, K. & Baker, J. C. Genomic evolution of the placenta using co-option and duplication and
848 divergence. *Genome Res* **18**, 695-705, doi:10.1101/gr.071407.107 (2008).
- 849 11 Sitras, V., Fenton, C., Paulssen, R., Vartun, A. & Acharya, G. Differences in gene expression
850 between first and third trimester human placenta: a microarray study. *PLoS One* **7**, e33294,
851 doi:10.1371/journal.pone.0033294 (2012).

- 852 12 Leavey, K., Bainbridge, S. A. & Cox, B. J. Large scale aggregate microarray analysis reveals three
853 distinct molecular subclasses of human preeclampsia. *PLoS One* **10**, e0116508,
854 doi:10.1371/journal.pone.0116508 (2015).
- 855 13 Simmons, D. G., Fortier, A. L. & Cross, J. C. Diverse subtypes and developmental origins of
856 trophoblast giant cells in the mouse placenta. *Dev Biol* **304**, 567-578,
857 doi:10.1016/j.ydbio.2007.01.009 (2007).
- 858 14 Cox, B. *et al.* Translational analysis of mouse and human placental protein and mRNA reveals
859 distinct molecular pathologies in human preeclampsia. *Mol Cell Proteomics* **10**, M111 012526,
860 doi:10.1074/mcp.M111.012526 (2011).
- 861 15 Soncin, F. *et al.* Comparative analysis of mouse and human placentae across gestation reveals
862 species-specific regulators of placental development. *Development* **145**,
863 doi:10.1242/dev.156273 (2018).
- 864 16 Muzumdar, M. D., Tasic, B., Miyamichi, K., Li, L. & Luo, L. A global double-fluorescent Cre
865 reporter mouse. *Genesis* **45**, 593-605, doi:10.1002/dvg.20335 (2007).
- 866 17 Liu, Y. *et al.* Single-cell RNA-seq reveals the diversity of trophoblast subtypes and patterns of
867 differentiation in the human placenta. *Cell Res* **28**, 819-832, doi:10.1038/s41422-018-0066-y
868 (2018).
- 869 18 Turco, M. Y. *et al.* Trophoblast organoids as a model for maternal-fetal interactions during
870 human placentation. *Nature* **564**, 263-267, doi:10.1038/s41586-018-0753-3 (2018).
- 871 19 Vento-Tormo, R. *et al.* Single-cell reconstruction of the early maternal-fetal interface in
872 humans. *Nature* **563**, 347-353, doi:10.1038/s41586-018-0698-6 (2018).
- 873 20 Thordarson, G., Folger, P. & Talamantes, F. Development of a placental cell culture system for
874 studying the control of mouse placental lactogen II secretion. *Placenta* **8**, 573-585,
875 doi:10.1016/0143-4004(87)90028-2 (1987).
- 876 21 Sferruzzi-Perri, A. N., Sandovici, I., Constancia, M. & Fowden, A. L. Placental phenotype and
877 the insulin-like growth factors: resource allocation to fetal growth. *J Physiol* **595**, 5057-5093,
878 doi:10.1113/JP273330 (2017).
- 879 22 Amash, A., Holcberg, G., Sapir, O. & Huleihel, M. Placental secretion of interleukin-1 and
880 interleukin-1 receptor antagonist in preeclampsia: effect of magnesium sulfate. *J Interferon*
881 *Cytokine Res* **32**, 432-441, doi:10.1089/jir.2012.0013 (2012).
- 882 23 Denley, A., Cosgrove, L. J., Booker, G. W., Wallace, J. C. & Forbes, B. E. Molecular interactions
883 of the IGF system. *Cytokine Growth Factor Rev* **16**, 421-439, doi:10.1016/j.cytogfr.2005.04.004
884 (2005).

- 885 24 Ding, R. *et al.* Altered Matrix Metalloproteinases Expression in Placenta from Patients with
886 Gestational Diabetes Mellitus. *Chin Med J (Engl)* **131**, 1255-1258, doi:10.4103/0366-
887 6999.231530 (2018).
- 888 25 Melhem, H. *et al.* Placental secretion of apolipoprotein A1 and E: the anti-atherogenic impact
889 of the placenta. *Sci Rep* **9**, 6225, doi:10.1038/s41598-019-42522-1 (2019).
- 890 26 Rogenhofer, N. *et al.* Assessment of M2/ANXA5 haplotype as a risk factor in couples with
891 placenta-mediated pregnancy complications. *J Assist Reprod Genet* **35**, 157-163,
892 doi:10.1007/s10815-017-1041-0 (2018).
- 893 27 Petraglia, F. Inhibin, activin and follistatin in the human placenta--a new family of regulatory
894 proteins. *Placenta* **18**, 3-8, doi:10.1016/s0143-4004(97)90065-5 (1997).
- 895 28 Landers, K. A., Mortimer, R. H. & Richard, K. Transthyretin and the human placenta. *Placenta*
896 **34**, 513-517, doi:10.1016/j.placenta.2013.04.013 (2013).
- 897 29 Mason, R. W. Emerging functions of placental cathepsins. *Placenta* **29**, 385-390,
898 doi:10.1016/j.placenta.2008.02.006 (2008).
- 899 30 Simmons, D. G., Rawn, S., Davies, A., Hughes, M. & Cross, J. C. Spatial and temporal expression
900 of the 23 murine Prolactin/Placental Lactogen-related genes is not associated with their
901 position in the locus. *BMC Genomics* **9**, 352, doi:10.1186/1471-2164-9-352 (2008).
- 902 31 Troncoso, F. *et al.* Gestational diabetes mellitus is associated with increased pro-migratory
903 activation of vascular endothelial growth factor receptor 2 and reduced expression of vascular
904 endothelial growth factor receptor 1. *PLoS One* **12**, e0182509,
905 doi:10.1371/journal.pone.0182509 (2017).
- 906 32 Bourque, D. K., Avila, L., Penaherrera, M., von Dadelszen, P. & Robinson, W. P. Decreased
907 placental methylation at the H19/IGF2 imprinting control region is associated with
908 normotensive intrauterine growth restriction but not preeclampsia. *Placenta* **31**, 197-202,
909 doi:10.1016/j.placenta.2009.12.003 (2010).
- 910 33 Nawathe, A. R. *et al.* Insulin-like growth factor axis in pregnancies affected by fetal growth
911 disorders. *Clin Epigenetics* **8**, 11, doi:10.1186/s13148-016-0178-5 (2016).
- 912 34 Tran, N. T. *et al.* Maternal citrulline supplementation enhances placental function and fetal
913 growth in a rat model of IUGR: involvement of insulin-like growth factor 2 and angiogenic
914 factors. *J Matern Fetal Neonatal Med* **30**, 1906-1911, doi:10.1080/14767058.2016.1229768
915 (2017).
- 916 35 Su, R. *et al.* Alteration in Expression and Methylation of IGF2/H19 in Placenta and Umbilical
917 Cord Blood Are Associated with Macrosomia Exposed to Intrauterine Hyperglycemia. *PLoS*
918 *One* **11**, e0148399, doi:10.1371/journal.pone.0148399 (2016).

919 36 Kappil, M. A. *et al.* Placental expression profile of imprinted genes impacts birth weight.
920 *Epigenetics* **10**, 842-849, doi:10.1080/15592294.2015.1073881 (2015).

921 37 Machado, J. S. R. *et al.* Role of plasma PIGF, PDGF-AA, ANG-1, ANG-2, and the ANG-1/ANG-2
922 ratio as predictors of preeclampsia in a cohort of pregnant women. *Pregnancy Hypertens* **16**,
923 105-111, doi:10.1016/j.preghy.2019.03.011 (2019).

924 38 Loegl, J. *et al.* GDM alters paracrine regulation of fetoplacental angiogenesis via the
925 trophoblast. *Lab Invest* **97**, 409-418, doi:10.1038/labinvest.2016.149 (2017).

926 39 Chui, A. *et al.* Expression of Biglycan in First Trimester Chorionic Villous Sampling Placental
927 Samples and Altered Function in Telomerase-Immortalized Microvascular Endothelial Cells.
928 *Arterioscler Thromb Vasc Biol* **37**, 1168-1179, doi:10.1161/ATVBAHA.117.309422 (2017).

929 40 Wang, Y., Tasevski, V., Wallace, E. M., Gallery, E. D. & Morris, J. M. Reduced maternal serum
930 concentrations of angiopoietin-2 in the first trimester precede intrauterine growth restriction
931 associated with placental insufficiency. *Bjog* **114**, 1427-1431, doi:10.1111/j.1471-
932 0528.2007.01511.x (2007).

933 41 Leavey, K. *et al.* Unsupervised Placental Gene Expression Profiling Identifies Clinically Relevant
934 Subclasses of Human Preeclampsia. *Hypertension* **68**, 137-147,
935 doi:10.1161/HYPERTENSIONAHA.116.07293 (2016).

936 42 Yung, H. W. *et al.* Placental endoplasmic reticulum stress in gestational diabetes: the potential
937 for therapeutic intervention with chemical chaperones and antioxidants. *Diabetologia* **59**,
938 2240-2250, doi:10.1007/s00125-016-4040-2 (2016).

939 43 Walentowicz-Sadlecka, M. *et al.* Assessment of the sFlt-1 and sFlt-1/25(OH)D Ratio as a
940 Diagnostic Tool in Gestational Hypertension (GH), Preeclampsia (PE), and Gestational Diabetes
941 Mellitus (GDM). *Dis Markers* **2019**, 5870239, doi:10.1155/2019/5870239 (2019).

942 44 Lappas, M. Markers of endothelial cell dysfunction are increased in human omental adipose
943 tissue from women with pre-existing maternal obesity and gestational diabetes. *Metabolism*
944 **63**, 860-873, doi:10.1016/j.metabol.2014.03.007 (2014).

945 45 Zhao, B., Han, X., Meng, Q. & Luo, Q. Early second trimester maternal serum markers in the
946 prediction of gestational diabetes mellitus. *J Diabetes Investig* **9**, 967-974,
947 doi:10.1111/jdi.12798 (2018).

948 46 Toso, C., Emamullee, J. A., Merani, S. & Shapiro, A. M. The role of macrophage migration
949 inhibitory factor on glucose metabolism and diabetes. *Diabetologia* **51**, 1937-1946,
950 doi:10.1007/s00125-008-1063-3 (2008).

951 47 Birdir, C. *et al.* Predictive value of sFlt-1, PlGF, sFlt-1/PlGF ratio and PAPP-A for late-onset
952 preeclampsia and IUGR between 32 and 37 weeks of pregnancy. *Pregnancy Hypertens* **12**, 124-
953 128, doi:10.1016/j.preghy.2018.04.010 (2018).

954 48 Pringle, K. G., Kind, K. L., Sferruzzi-Perri, A. N., Thompson, J. G. & Roberts, C. T. Beyond oxygen:
955 complex regulation and activity of hypoxia inducible factors in pregnancy. *Hum Reprod Update*
956 **16**, 415-431, doi:10.1093/humupd/dmp046 (2010).

957 49 Than, N. G. *et al.* Integrated Systems Biology Approach Identifies Novel Maternal and Placental
958 Pathways of Preeclampsia. *Front Immunol* **9**, 1661, doi:10.3389/fimmu.2018.01661 (2018).

959 50 Jansson, D. *et al.* Glucose controls CREB activity in islet cells via regulated phosphorylation of
960 TORC2. *Proc Natl Acad Sci U S A* **105**, 10161-10166, doi:10.1073/pnas.0800796105 (2008).

961 51 Whitehead, C. L. *et al.* Identifying late-onset fetal growth restriction by measuring circulating
962 placental RNA in the maternal blood at 28 weeks' gestation. *Am J Obstet Gynecol* **214**, 521
963 e521-521 e528, doi:10.1016/j.ajog.2016.01.191 (2016).

964 52 Lopez-Tello, J. *et al.* Fetal and trophoblast PI3K p110alpha have distinct roles in regulating
965 resource supply to the growing fetus in mice. *Elife* **8**, doi:10.7554/eLife.45282 (2019).

966 53 Hensen, K. *et al.* Targeted disruption of the murine Plag1 proto-oncogene causes growth
967 retardation and reduced fertility. *Dev Growth Differ* **46**, 459-470, doi:10.1111/j.1440-
968 169x.2004.00762.x (2004).

969 54 Nielsen, H., Tsirigos, K. D., Brunak, S. & von Heijne, G. A Brief History of Protein Sorting
970 Prediction. *Protein J* **38**, 200-216, doi:10.1007/s10930-019-09838-3 (2019).

971 55 Grimmond, S. M. *et al.* The mouse secretome: functional classification of the proteins secreted
972 into the extracellular environment. *Genome Res* **13**, 1350-1359, doi:10.1101/gr.983703
973 (2003).

974 56 Meek, C. *et al.* Approaches to screening for hyperglycaemia in pregnant women during and
975 after the Covid-19 pandemic. *Diabetic Medicine*, doi:10.17863/CAM.54385 (2020).

976

977

Figures

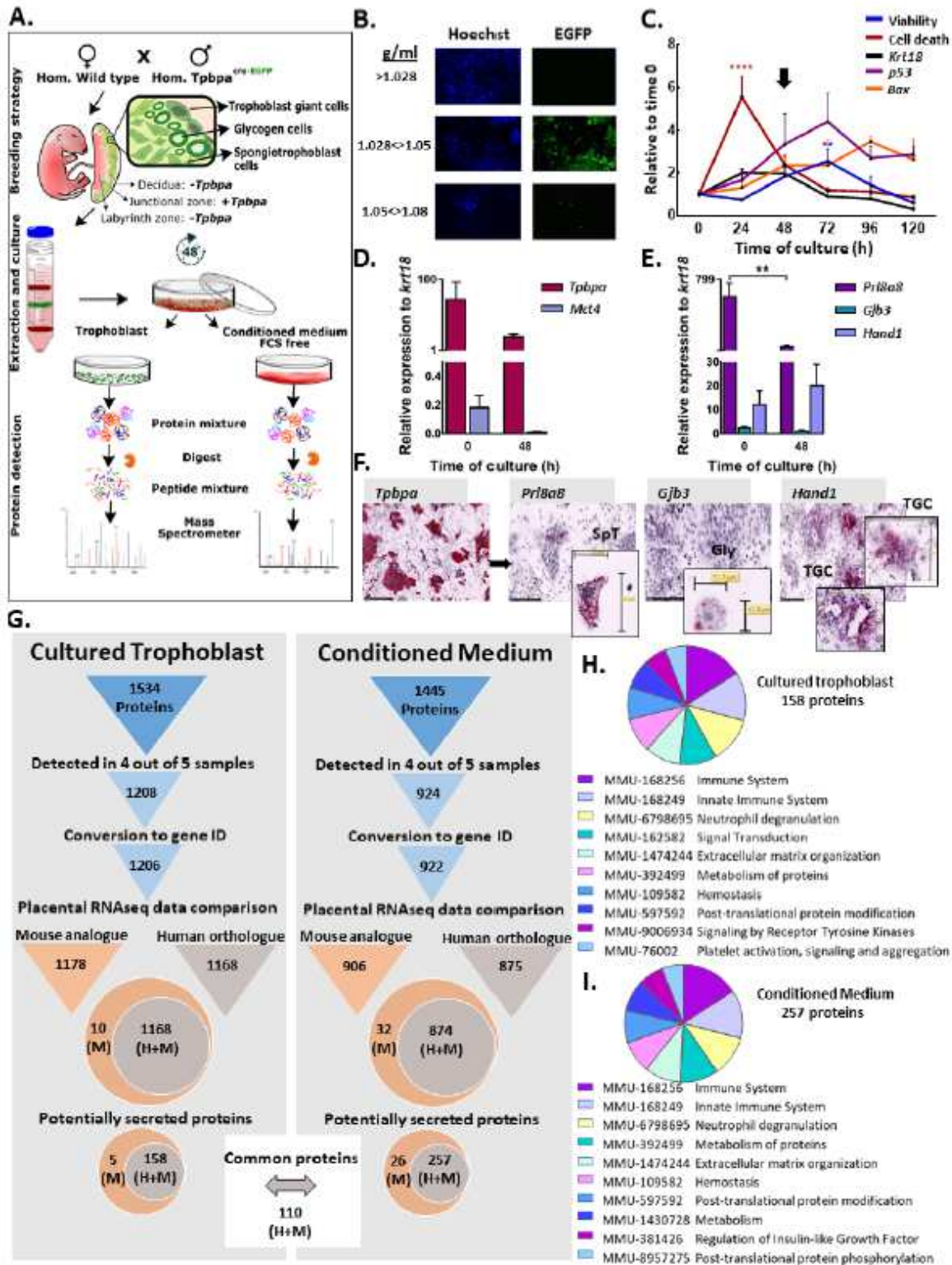


Figure 1

Detection of secreted proteins in primary cultures of mouse trophoblast. A) Workflow for the detection of secreted proteins in primary cultures of trophoblast from mice at day 16 of pregnancy. B) Visualisation of EGFP (*Tpbpa*-Cre-EGFP reporter) by fluorescence microscopy to identify the Percoll gradient layer

containing trophoblast endocrine cells. Cells in layers were counterstained with Hoechst dye (blue) and photographed at magnification 10X (scale bar-0.6mm). C) Primary cell culture viability (determined by XTT), cell death (LDH release levels), trophoblast density (Krt18 gene expression) and apoptosis (p53 and Bax gene expression) from time 0 to 120h. D) Proportion of junctional zone (Tpbpa gene expression) and labyrinthine zone (Mct4 gene expression) trophoblast at 0h and 48h. E) Relative abundance of the three junctional zone endocrine cell types, spongiotrophoblast, glycogen cells and giant cells (gene expression of Prl8a8, Gjb3 and Hand1, respectively) at 0h and 48h of culture. F) Representative images of cells stained in situ using RNAscope probes against; Tpbpa, Prl8a8, Gjb3 and Hand1 to visualise trophoblast endocrine cells, spongiotrophoblast (SpT), glycogen cells (Gly) and giant cells (TGC), respectively. G) Pipeline and results of the analysis of proteins detected by mass spectrometry in cultured trophoblast and their conditioned medium including conversion to RNA sequences and overlay with published RNA data for the mouse and human placenta. Secreted proteins identified using SignalP and combined gene ontology (GO) terms: extracellular region, extracellular exosome, extracellular region parts and signal IP. H and I) Pathway over-representation analysis using Reactome pathway by STRING V.11 for the 158 and 257 secreted placental proteins in cultured trophoblast and their conditioned medium, respectively that are expressed by both mouse and human placenta. XTT, LDH and gene expression data relative to geometric mean of three housekeeping genes: Gapdh, RPII and Hprt are presented as mean \pm SEM and expressed relative to expression at time 0h. Asterisks denote statistical significance versus time 0h, using Two-way ANOVA (B) or t-test (C-D), **P<0.01, ****P<0.001, n=6-10 of 4 pooled litters.

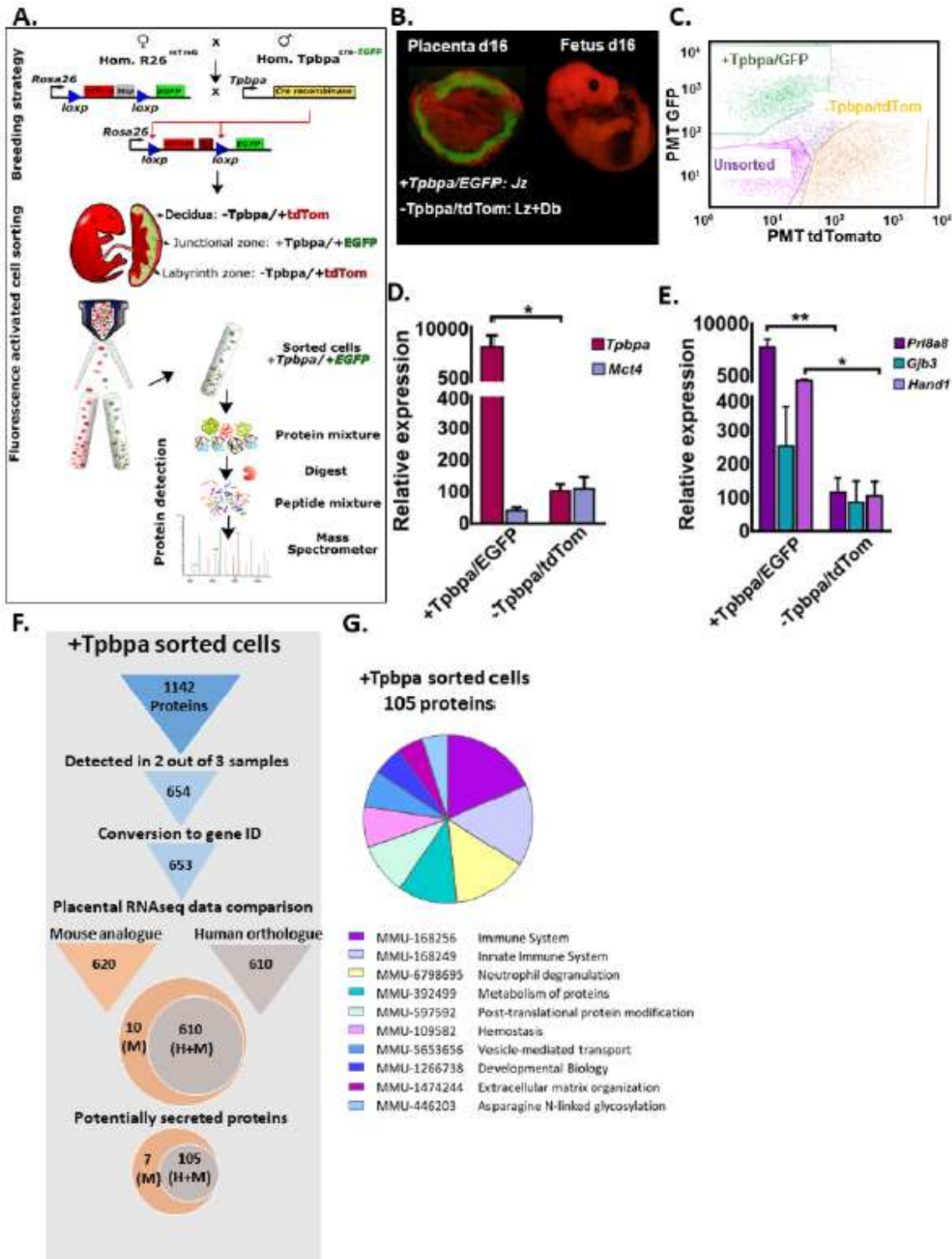


Figure 2

Detection of secreted proteins in sorted mouse trophoblast endocrine cells. A) Workflow for the cell sorting and protein expression analysis of mouse trophoblast endocrine cells from mice at day 16 of pregnancy. B) Fluorescent image of placenta showing EGFP in *Tpbpa* positive cells (junctional zone of the placenta) and tdTom for *Tpbpa* negative cells. C) Representative image of cell sorting of EGFP/tdTom cells by fluorescence activated cell sorting. D) Expression of junctional zone and labyrinth zone markers,

Tpbpa and Mct4, respectively in the EGFP and TdTom sorted cells. E) Expression of markers for junctional zone cell types, spongiotrophoblast cell (Pr18a8), glycogen cells (Gjb3) and giant cells (Hand1). F) Pipeline and results of the analysis of proteins detected by mass spectrometry in sorted Tpbpa+/EGFP cells. G) Pathway over-representation analysis using Reactome pathway by STRING V.11 for the 105 secreted placental proteins expressed by both mouse and human placenta. Data presented as mean \pm SEM and genes expressed relative to geometric mean of two housekeeping genes: RPII and Hprt. Asterisks denote statistical significance to the Tpbpa+/EGFP sorted cells, using t-test, *P<0.05, **P<0.01, n=5 for each group.

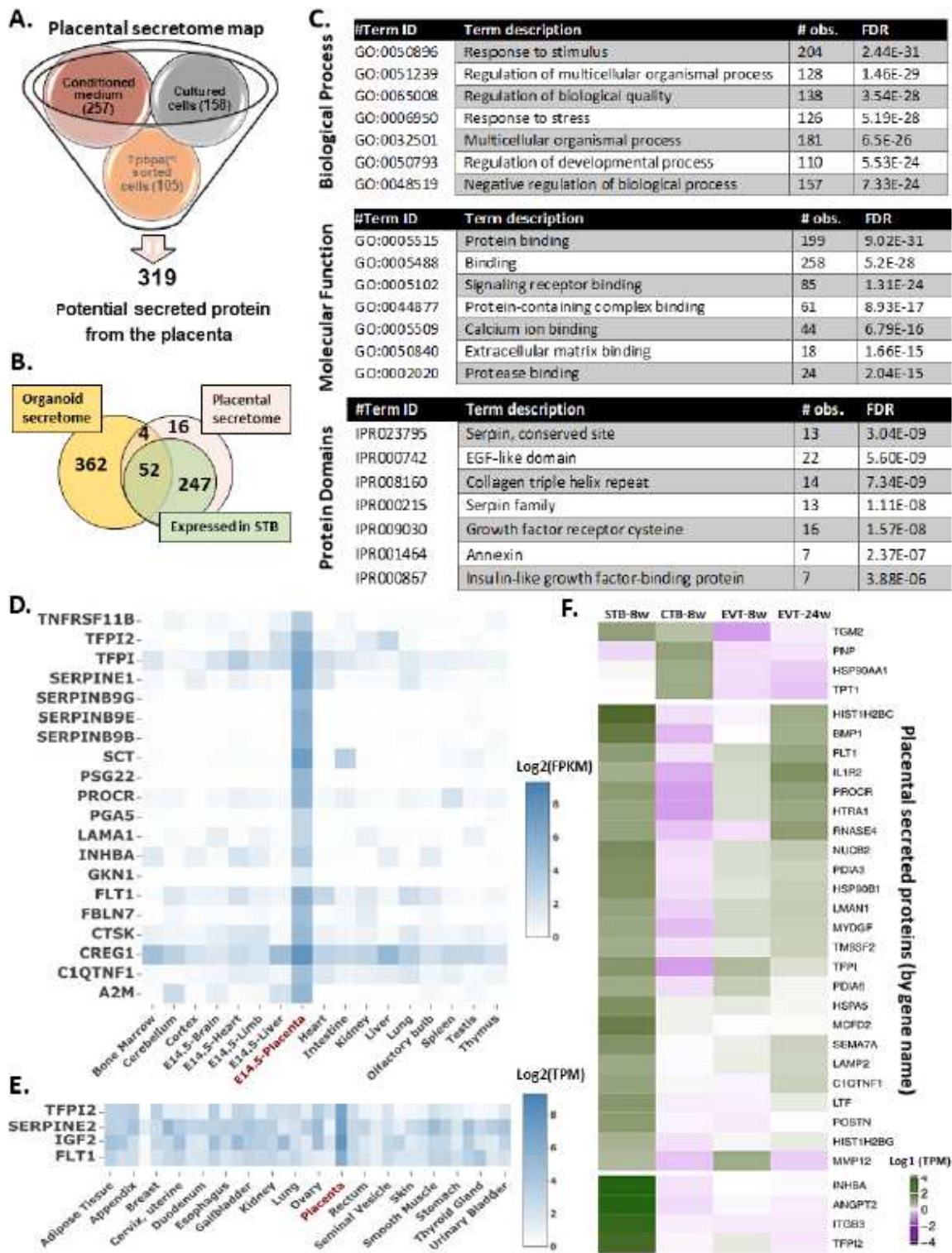


Figure 3

Secretome map of the placenta A) Integrating the lists of secreted placental proteins expressed by mouse and human placenta and obtained using our different methods to generate a comprehensive placental secretome map. Proteins expressed by mouse but not human placenta shown in Supplementary data figure 1. B) Venn diagram showing the overlay of placental secretome map with first trimester trophoblast organoid secretome (Turco, 2018) and single cell RNAseq analysis for human placenta at 8 weeks of

gestation (Liu, 2018). C) Gene ontology (GO) analysis for the 319 secreted proteins detected in placental secretome map using STRING V.11. D and E) Proteins in the placental secretome map that are highly enriched in the placenta of mouse (D) and human (E) compared to other tissues using TissueEnrich. F) Cell specific expression of the top 30 most highly expressed genes in the placental secretome map using single cell RNAseq data for the human placenta (see results text for details). CTB: cytotrophoblasts, STB: syncytiotrophoblast, EVT: extravillous trophoblasts, w: weeks.

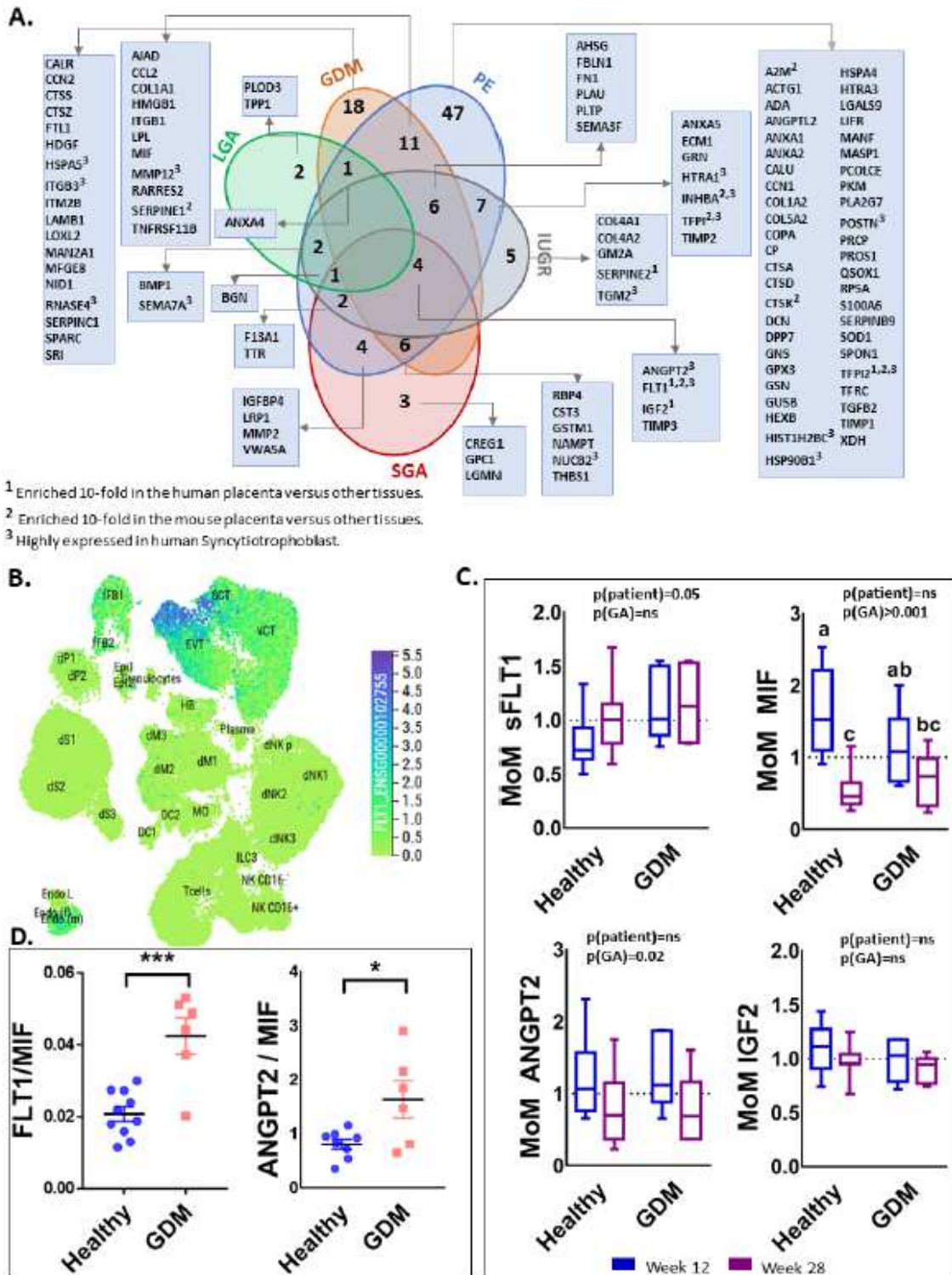


Figure 4

Applying the secretome map of the placenta to data available for human pregnancy complications. A) Venn diagram showing the number of placental proteins in the secretome map that are differentially expressed in the placenta of women with a pregnancy complication. B) FLT1 expression at the maternal-fetal interface of early human pregnancy via the CellxGene tool (<https://maternal-fetal-interface.cellgeni.sanger.ac.uk/>). C) Serum levels of FLT1, MIF, ANGP2 and IGF2 in pregnant women at 12 and 28 weeks of gestation who went on to have normoglycemic (healthy) pregnancies or developed GDM. Data are expressed as multiple for the median; MoM. D) Ratio of the levels of FLT1 to MIF and ANGPT2 to MIF at week 12 of pregnancy in healthy women and those who went on to develop GDM. Data are presented as mean \pm SEM of MoM. Raw data for proteins levels are shown in supplementary figure 4. Asterisks denote statistical significance to the GDM pregnancies, using two way-ANOVA for C and t-test for D, *P<0.05, **P<0.01, n=10-11 for healthy pregnancies, n=6 for GDM. GDM: gestational diabetes mellitus, IUGR: intrauterine growth restriction, LGA: large for gestational age, PE: preeclampsia, SGA small for gestational age.

A.

TF	Motif	IPA (p value)	AME (adjusted p value)	Common (DEG in pathology complications)	Complications (TF as DEG)	Reference
ARNT2		14/319 (1.71E-06)	174/319 (1.30E-13)	10 (5)	PE SGA	Leavey et al. 2015 Sober et al. 2015
ELF3		3/319 (1.04E-02)	161/319 (5.07E-08)	2 (2)	PE IUGR	Sober et al. 2015
PLAG1		3/319 (4.34E-02)	185/319 (1.82E-04)	2 (1)	GDM	Sober et al. 2015
SP2		2/319 (1.87E-02)	166/319 (2.45E-01)	2 (1)	IUGR LGA PE	Sober et al. 2015
MEF2D		6/319 (5.59E-04)	124/319 (3.84E-23)	4 (3)	IUGR PE	Sober et al. 2015
MYCN		25/319 (5.51E-13)	71/319 (1.40E-08)	2 (2)	PE	Leavey et al. 2015
FOS		49/319 (4.45E-24)	41/319 (1.37E-02)	7 (3)	PE	Gormley et al. 2017
NFYC		4/319 (2.93E-03)	38/319 (7.54E-10)	2 (1)	PE	Leavey et al. 2015
CREB1		22/319 (2.69E-05)	10/319 (1.83E-02)	2 (2)	GDM	Bari et al. 2016
IRF3		9/319 (8.50E-03)	162/319 (5.83E-04)	6 (3)	GDM PE	Sober et al. 2015 Leavey et al. 2015

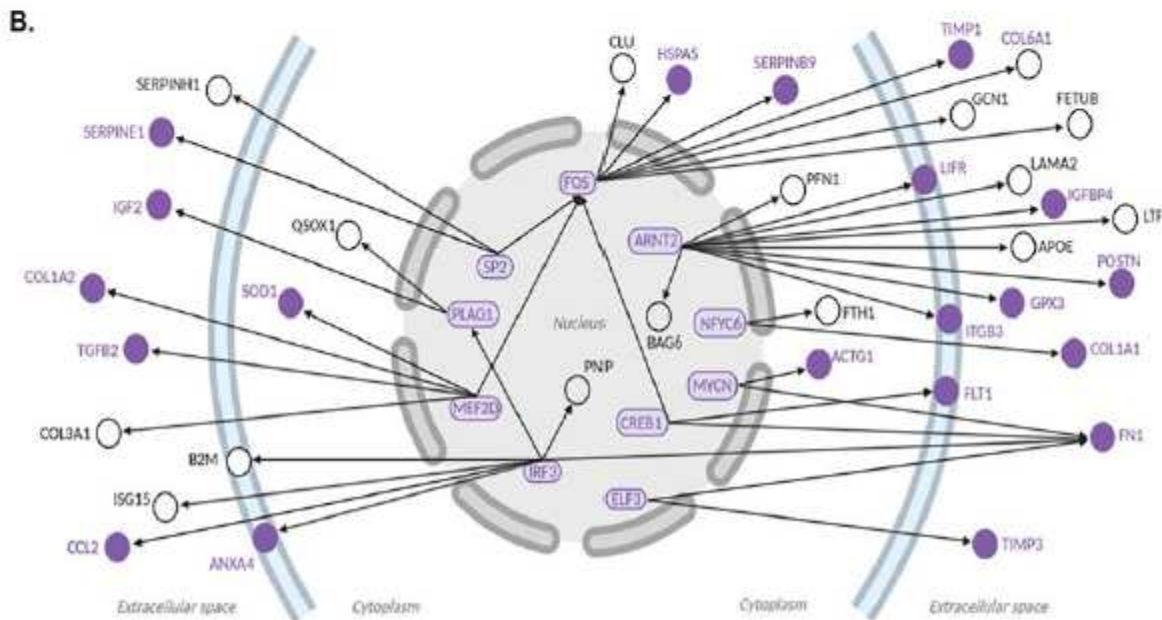


Figure 5

Transcription factors dysregulated in pregnancy complications identified as possible regulators of genes encoding secreted placental proteins. A) Table showing the ten transcription factors with altered expression in pregnancy complications and with binding sites enriched at the promoters of genes encoding proteins in the placental secretome map. B) Regulatory network built with the ten transcription factors listed in panel A. The ten transcription factors and their targets that are differentially expressed in

pregnancy complications are highlighted in purple. Location of the target proteins is according to their main cellular/extracellular compartment indicated by IPA. The graph was generated using BioRender.

Supplementary Files

This is a list of supplementary files associated with this preprint. Click to download.

- [SupplementaryMaterialsCombiology1.pdf](#)